

# Strain Accumulation Visco-Elastic Ventriculomegaly Hypothesis for the onset of idiopathic Normal Pressure Hydrocephalus (iNPH): in search of the molecular culprits.

Juan C. Lasheras, Ph.D.  
Institute of Engineering in Medicine  
MAE and Bioengineering Departments  
University of California San Diego  
La Jolla, CA 92093  
[jlasheras@eng.ucsd.edu](mailto:jlasheras@eng.ucsd.edu)



National Institute of  
General Medical Sciences



# Strain Accumulation Visco-Elastic Ventriculomegaly Hypothesis for the onset of idiopathic Normal Pressure Hydrocephalus (iNPH)

- Some relevant Anatomical and Physiological considerations.
- idiopathic **Normal Pressure Hydrocephalus (iNPH)**
- Measurement of Brain Viscoelastic Properties using Magnetic Resonant Elastography(MRE)
- Proof of concept simplified geometry
- Take Home message and concluding thoughts

# Cerebrospinal fluid (CSF)

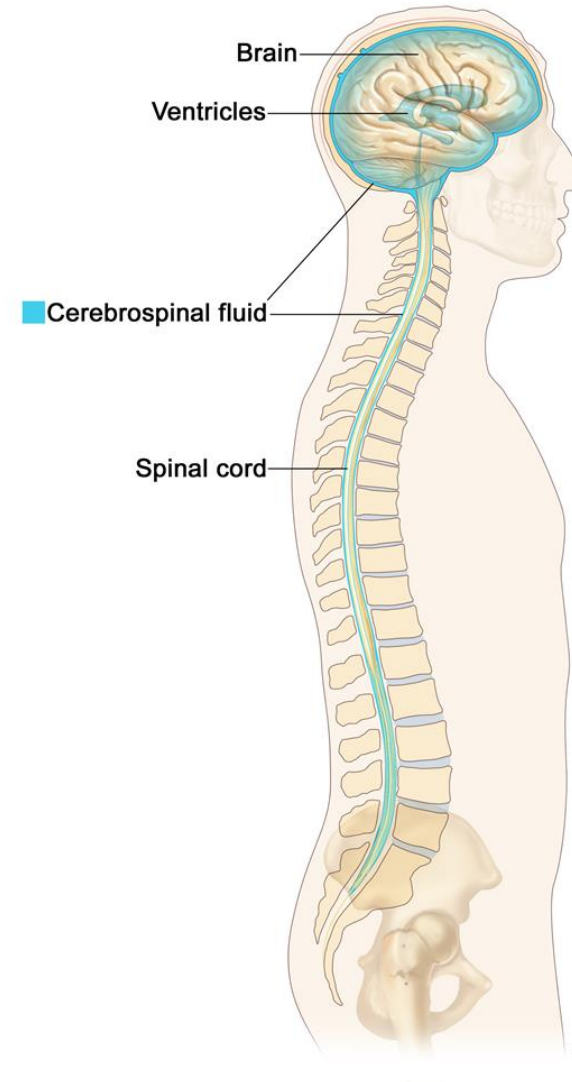
The entire surface of central nervous system is bathed by a clear, colorless fluid called **cerebrospinal fluid (CSF)**

The CSF is largely similar to blood plasma, except that is nearly protein-free compared with plasma and has modified electrolyte levels.

Healthy cerebrospinal fluid is free of red blood cells and contains only a few white blood cells.

Protein and cell concentration in CSF does not significantly affect its viscosity.

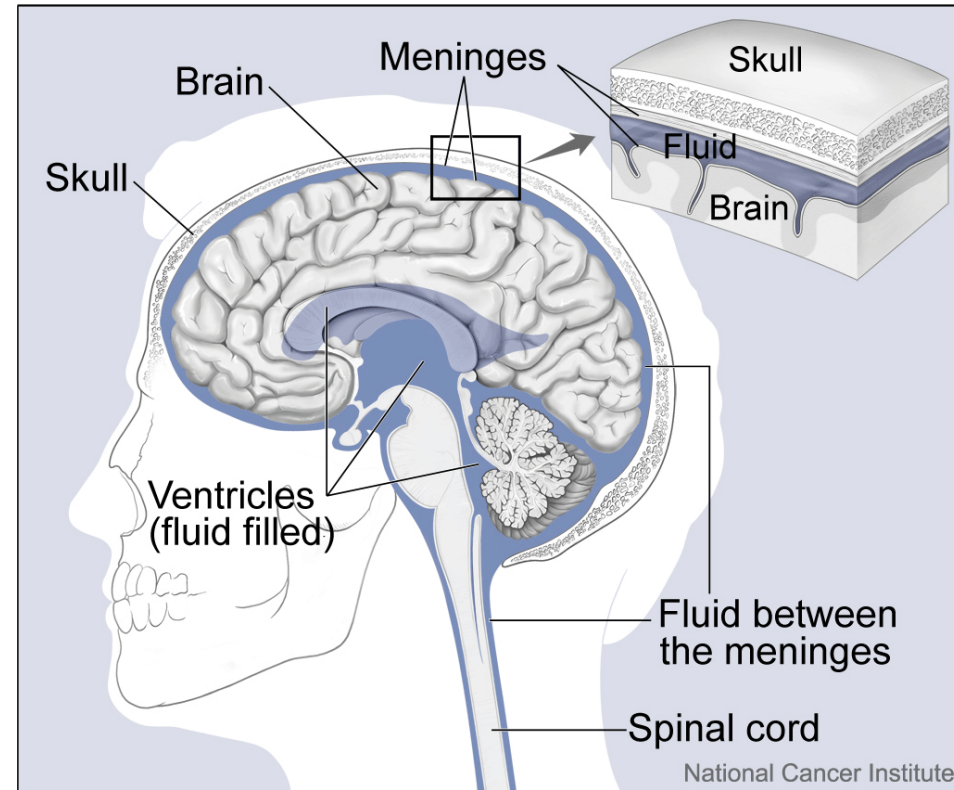
CSF is a **Newtonian fluid**, and its viscosity and density at 37 C are very similar to those of water.



# CSF Plays a Dual Mechanical and Physiological Function

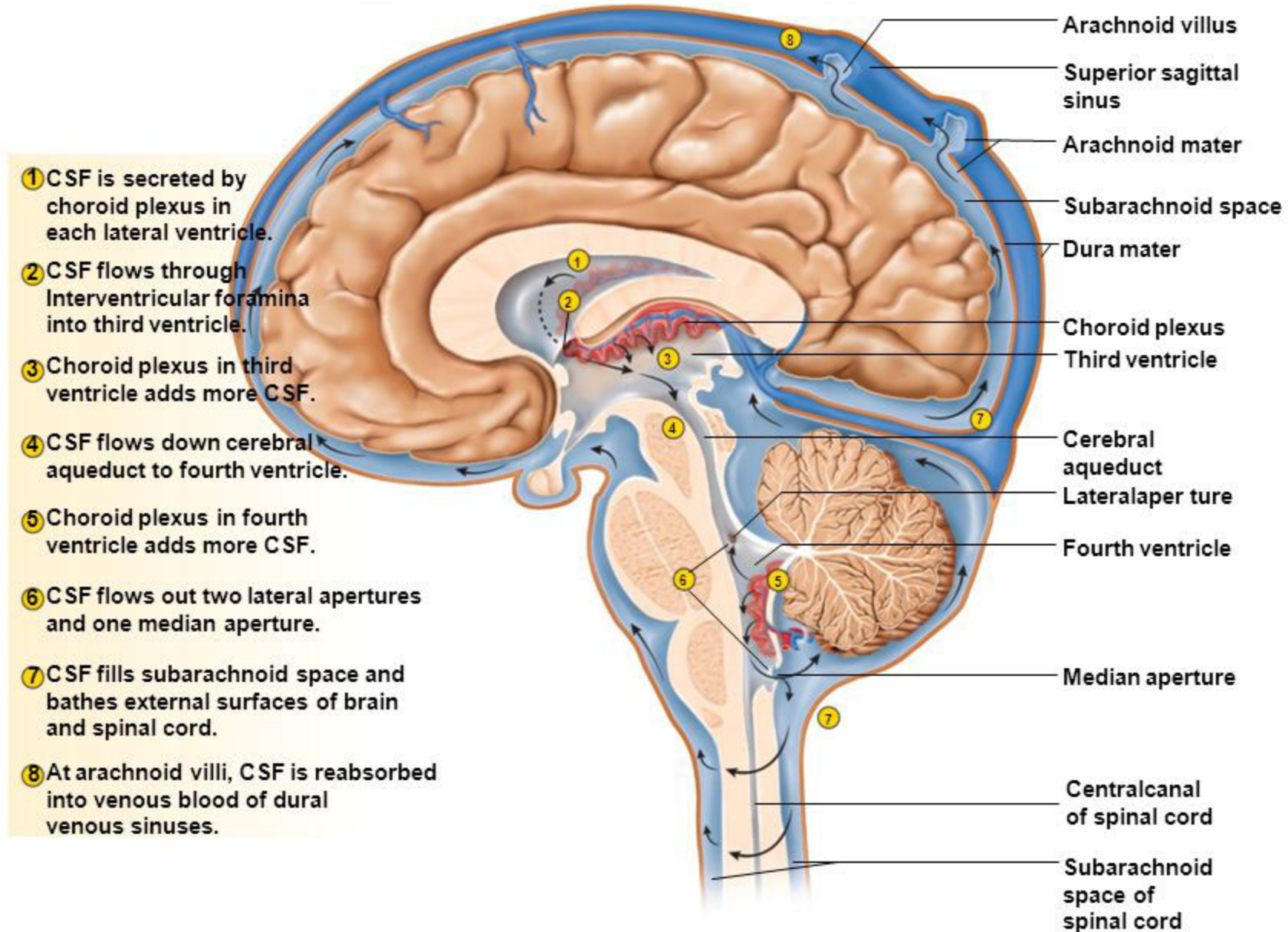
The primary **mechanical function** of CSF is to cushion the brain within the skull and serve as a **shock absorber** for the central nervous system.

A typical brain in air weighs 1400 gr. Due to **buoyancy** effects the pull of gravity only exerts a force equivalent to 50gr. Therefore, the **pressure at the base of the brain is drastically reduced**.

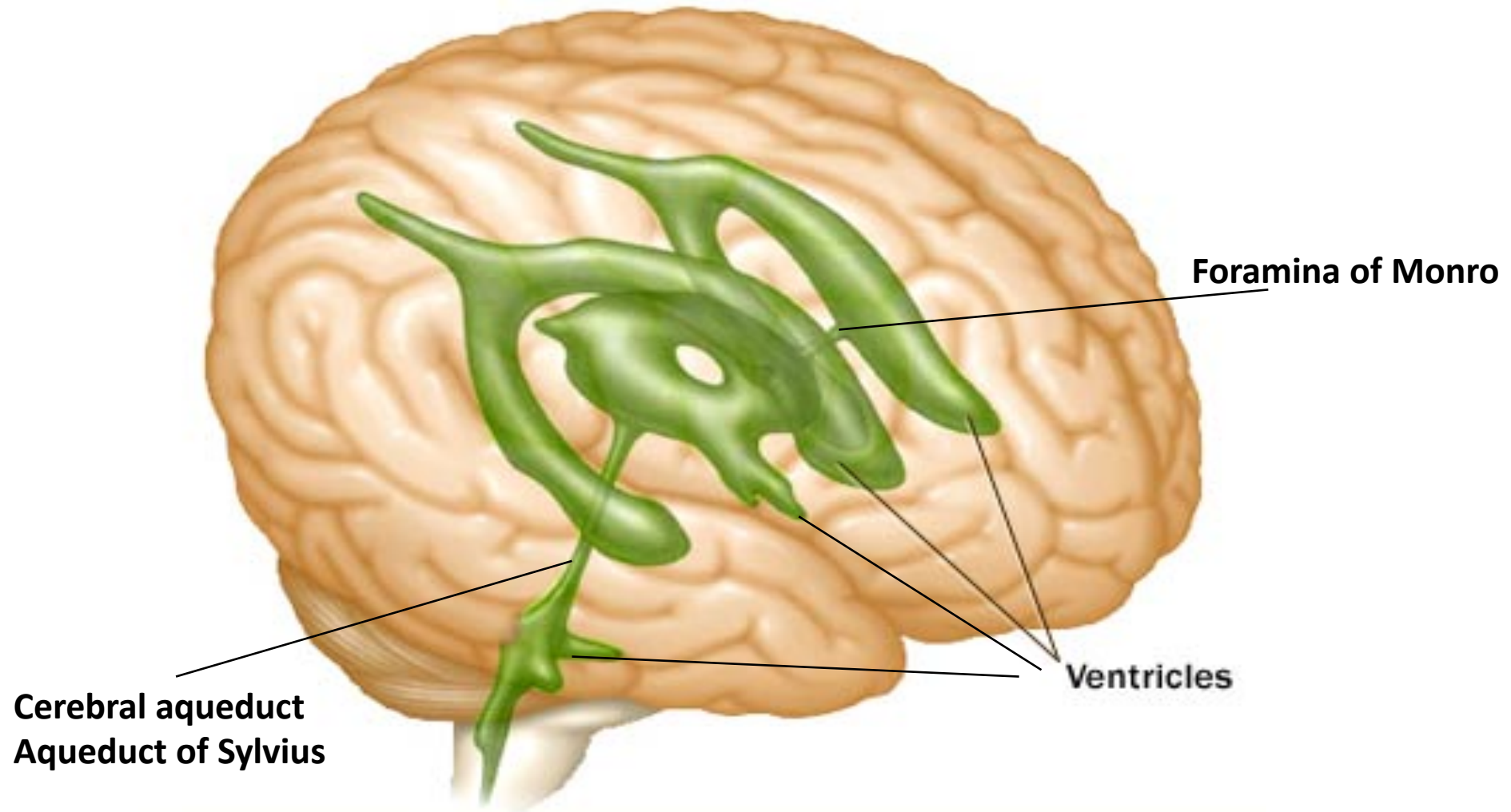


**CSF also plays an important physiological function:** maintains the electrolyte level, circulates nutrients and chemicals filtered from the blood, removes waste products, transports hormones, neurotransmitters, and other neuropeptides throughout the Brain and Central Nervous System (CNS).

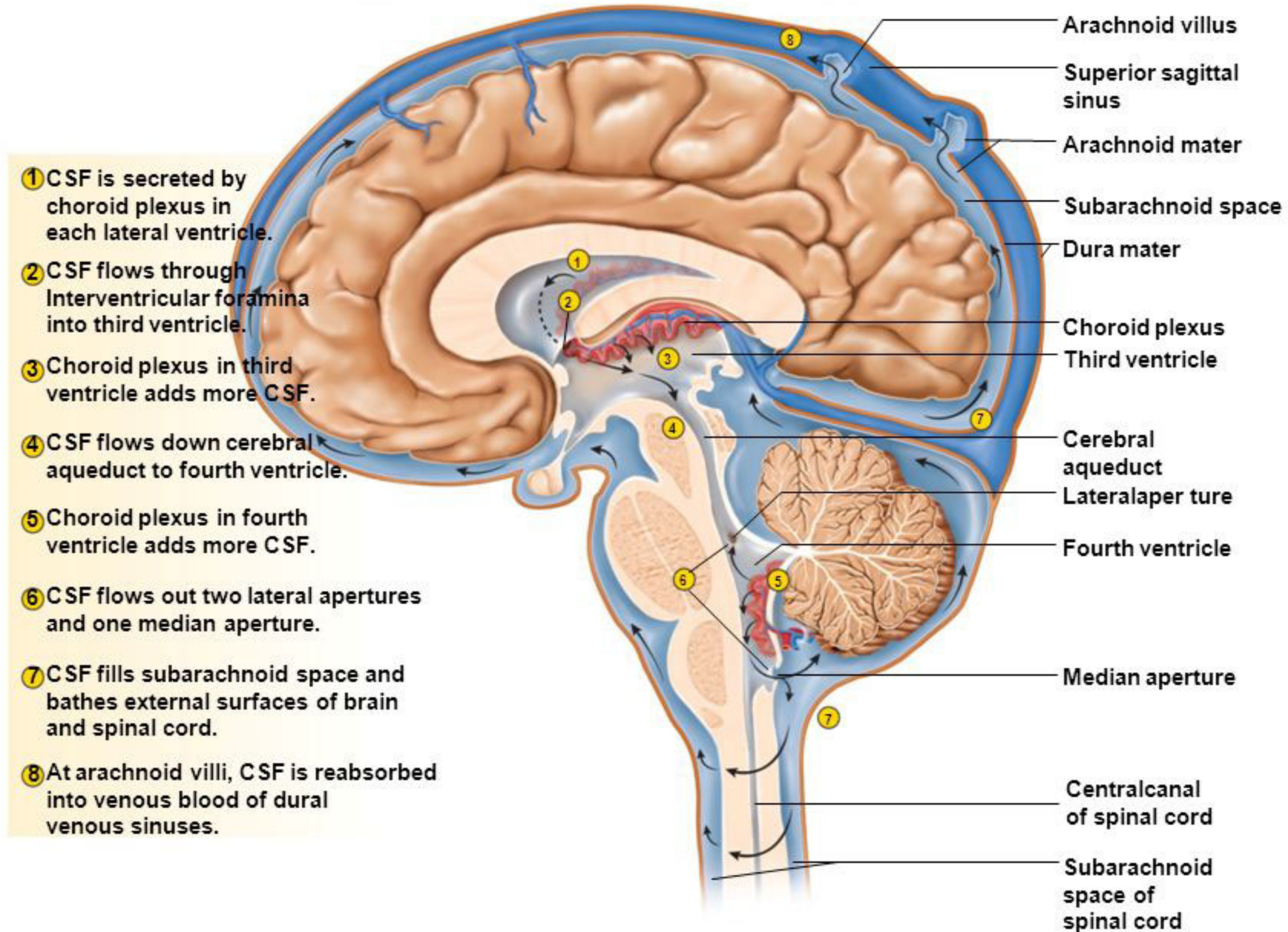
# Cerebrospinal Fluid



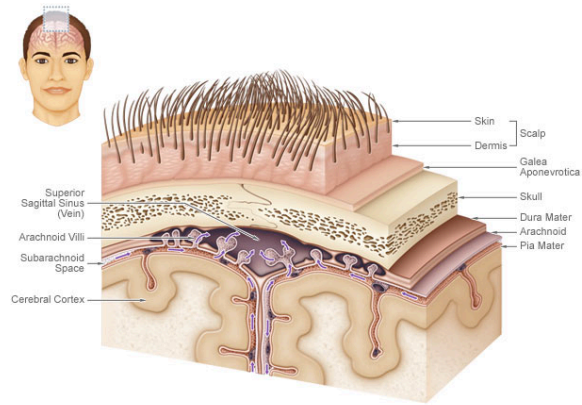
# Brain Ventricles



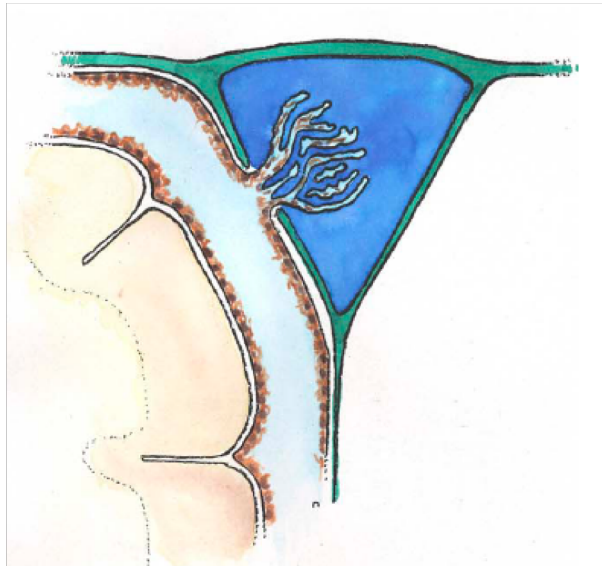
# Cerebrospinal Fluid



# Cerebrospinal Fluid



© Sophyssa - Illustration: Philippe Plateaux



CSF is primarily absorbed across the arachnoid villi into the venous circulation.

It probably also drains into olfactory mucosa, cranial nerve sheaths (optic, trigeminal, and facial nerves), and lymphatic vessels around the cranial cavity.

All of these are **pressure driven filtration processes**

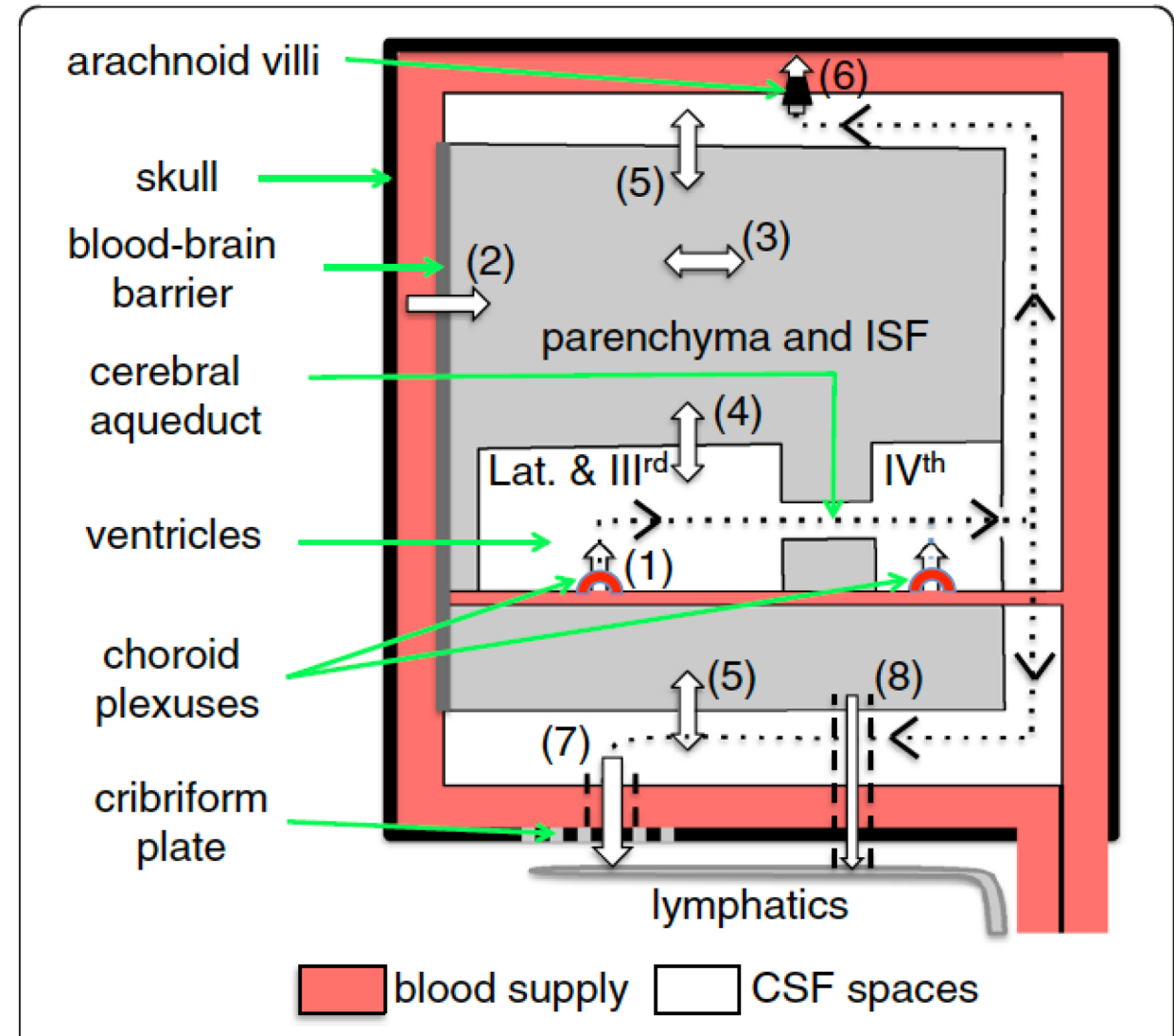
Secretion into the ventricles across the choroid plexuses (1) and into the brain parenchyma across the blood-brain barrier (2).

Fluid components can move through the parenchyma (3)

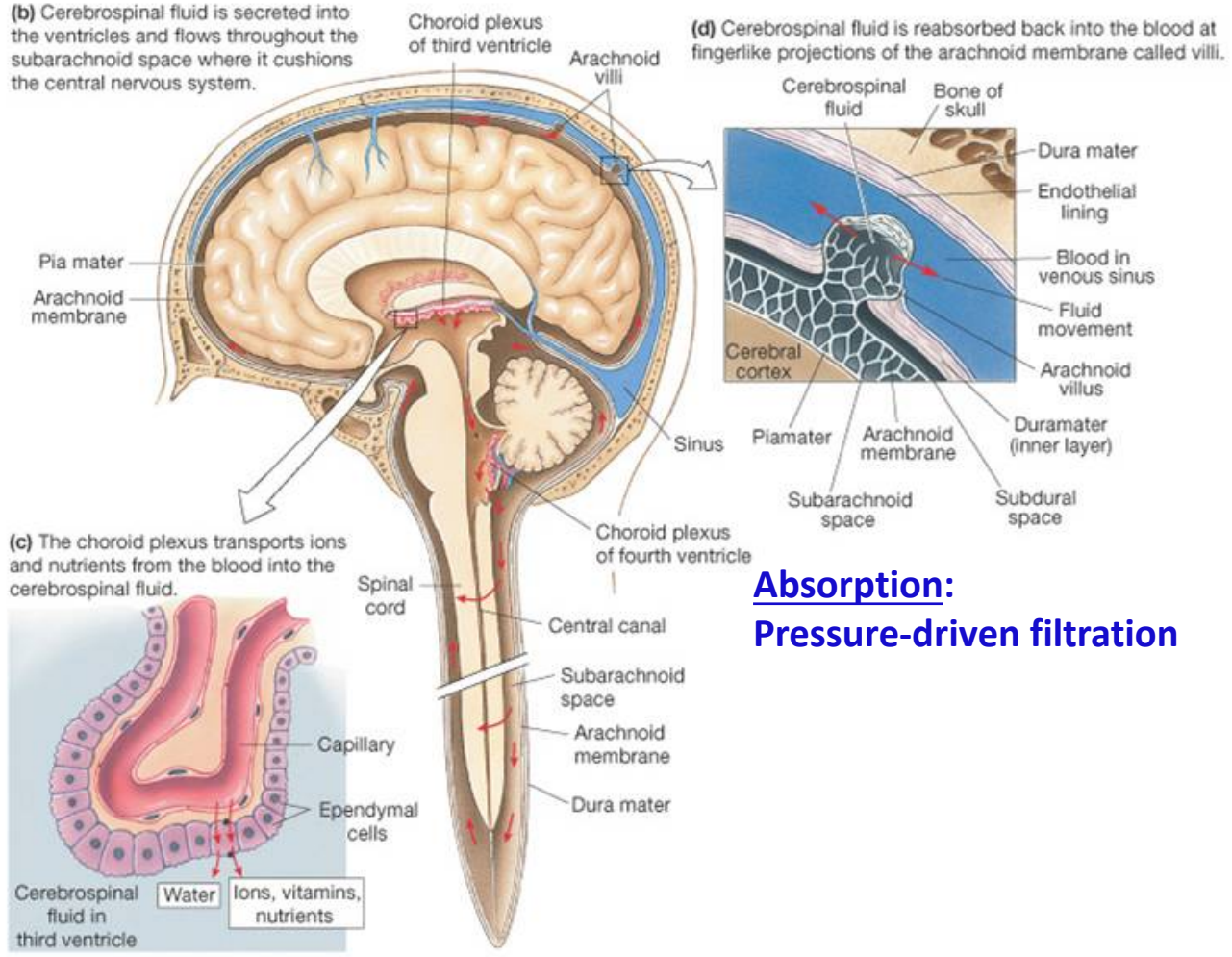
Exchanges of water and solutes (4) and (5) between the interstitial fluid (ISF) and cerebrospinal fluid (CSF) in the ventricles and in the subarachnoid spaces.

Net fluid outflow across the arachnoid villi (6) and along cranial nerves mainly olfactory nerve leading to the cribriform plate (7) and thence to the nasal mucosa.

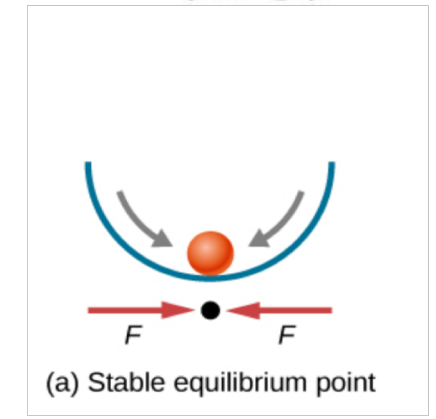
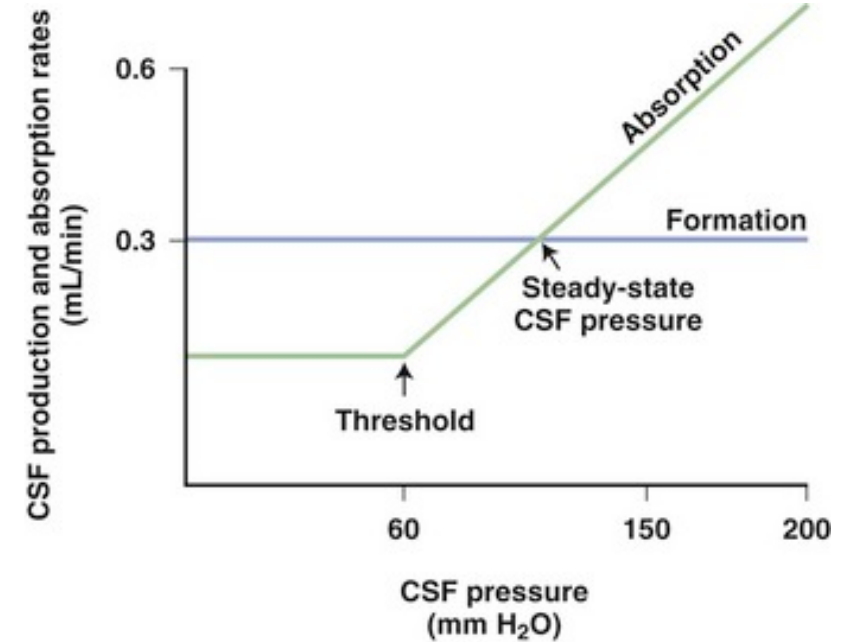
There may also be outflow in the perivascular spaces (Virchow–Robin spaces) (8) leading to a lymphatic drainage system.



# Cerebrospinal Fluid



**Absorption:**  
**Pressure-driven filtration**



**Secretion:** Ependymal cells secrete sodium ions into the lateral ventricles. This creates osmotic pressure and draws water into the CSF space.

# Infant Hydrocephalus

## Etiology of Hydrocephalus

Impaired absorption

Meningitis

Intraventricular hemorrhage

Congenital reduced number of arachnoid villi

Arachnoiditis

Choroid plexus papilloma

Choroid plexus carcinoma

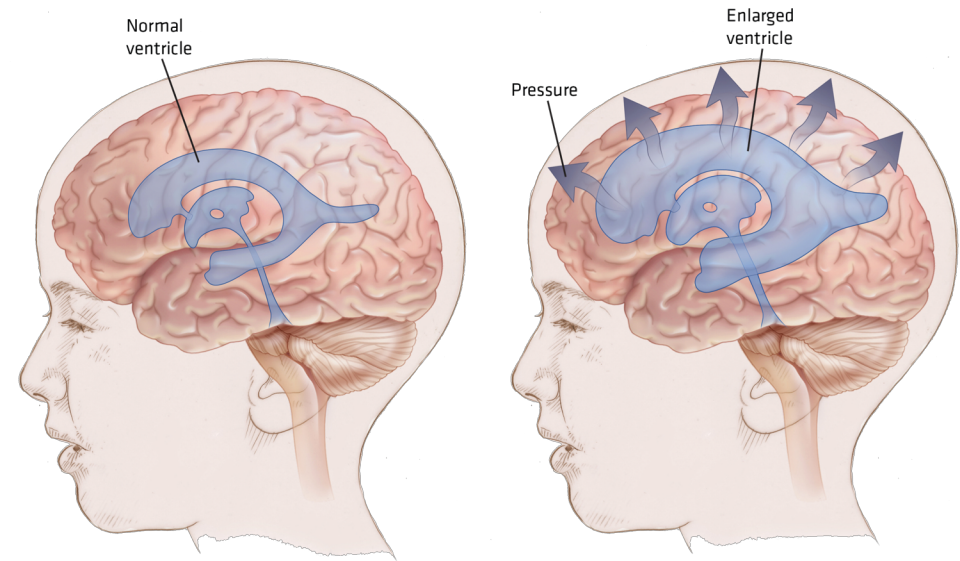
Obstruction – congenital causes

Aqueductal stenosis

Arnold chiari malformation

Tumors

Subarachnoid hemorrhage

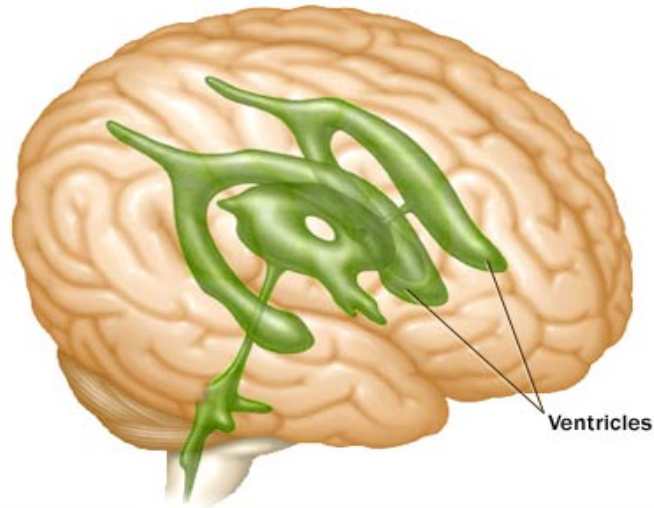


The amount of CSF increase when:

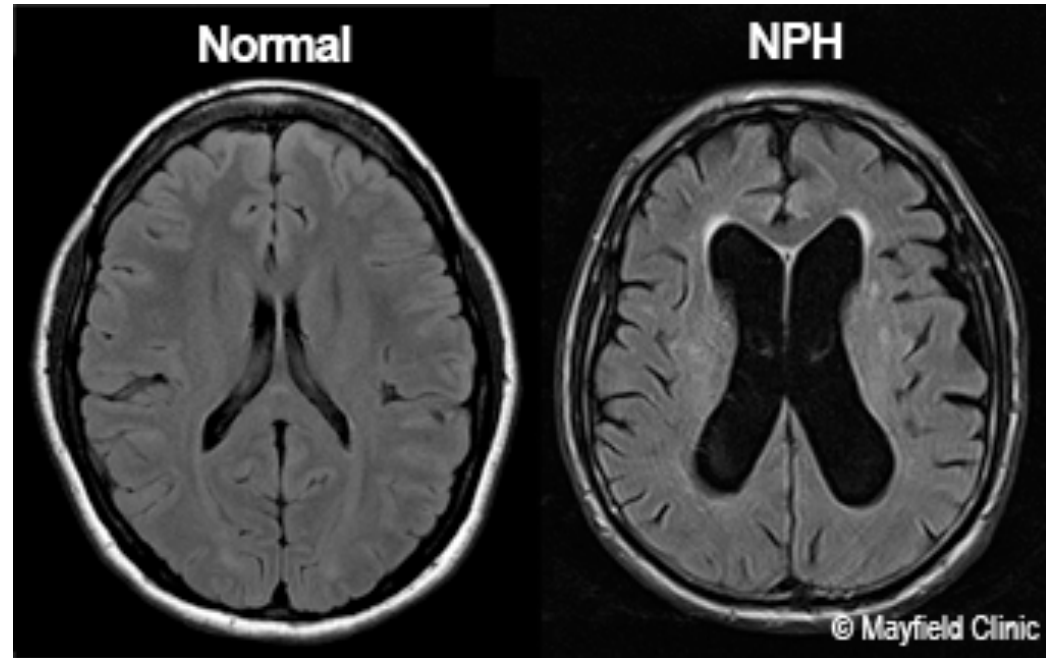
1. a blockage develops that prevents CSF from flowing normally, or
2. there is a decrease in the ability of blood vessels to absorb it

The **intracranial pressure increases** causing swelling of the skull.

# Idiopathic Communicating Normal Pressure Hydrocephalus (iNPH)

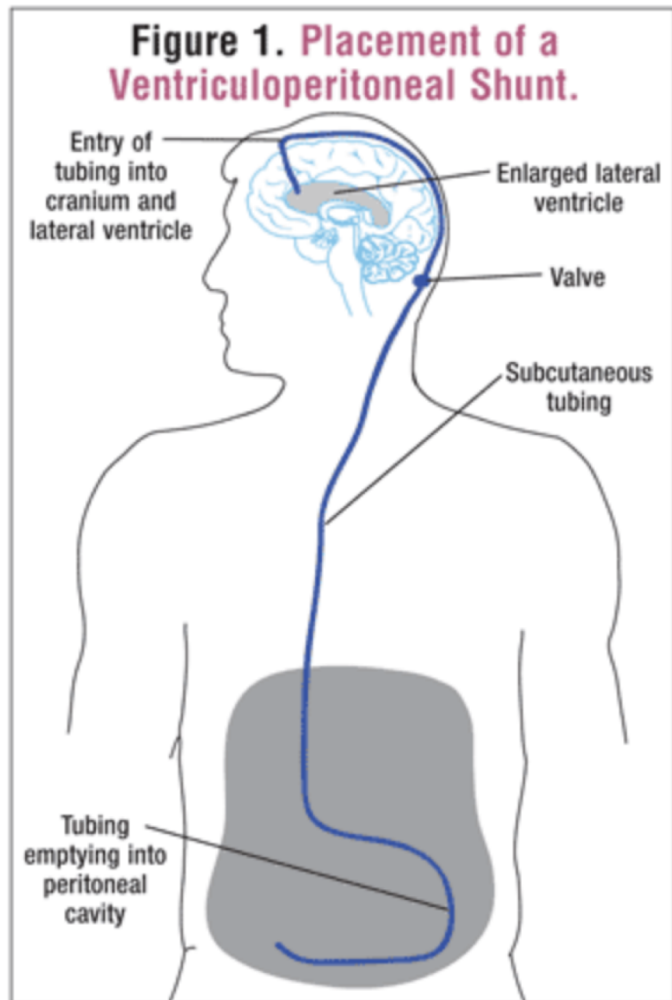


© Mayo Foundation for Medical Education and Research. All rights reserved.



- iNPH also referred to as Chronic Adult Hydrocephalus or Hakim’s Disease. Originally described in the mid 1960s is a syndrome characterized by ventriculomegaly in the absence of elevated intracranial pressure (ICP).
- Commonly characterized by a triad symptoms: urinary incontinence (loss of bladder control), disturbed gait, and dementia.
- iNPH is most common in the elderly population. The prevalence iNPH is estimated to be 0.2% in those aged 70–79 years increasing to 5.9% in those aged 80 years and older, with no difference between men and women.
- iNPH appears to be **extremely underdiagnosed**. Prevalence may be higher in assisted-living and extended-care residents, with as many as 12% of patients fulfilling the criteria for suspected iNPH.

# Idiopathic normal pressure hydrocephalus (iNPH) is the only potentially reversible neurodegenerative disease.



- In 1965 Hakim and Adams originally described iNPH as a surgically treatable cause of dementia and since then is thought as a **“potentially reversible neurodegenerative disease”**.
- Shunting doesn't help everyone with iNPH, and there's uncertainty about how best to identify those most likely to benefit. There's also a lack of data showing how long the benefit of shunting may last for those whose symptoms improve.
- The iNPH progresses insidiously over long periods of time, presumably **over several months, or even years**.
- **There is a need to develop an early diagnosis to guide either the surgical or pharmacological intervention.**

**The cause of the communicating iNPH condition has been the subject of considerable studies but a consensus remains elusive.**

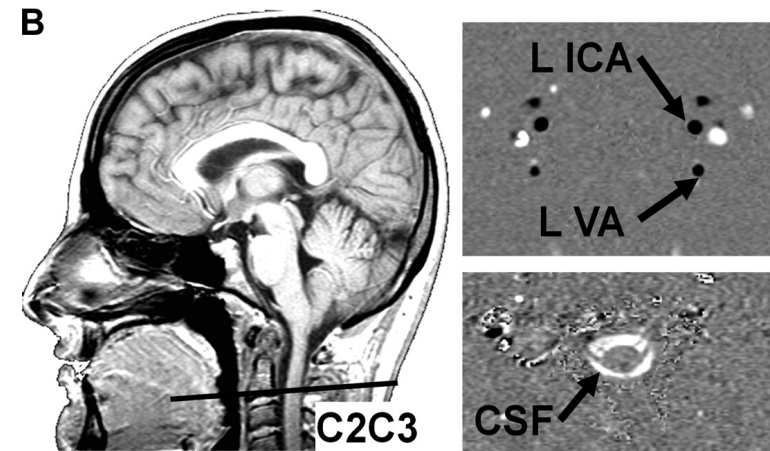
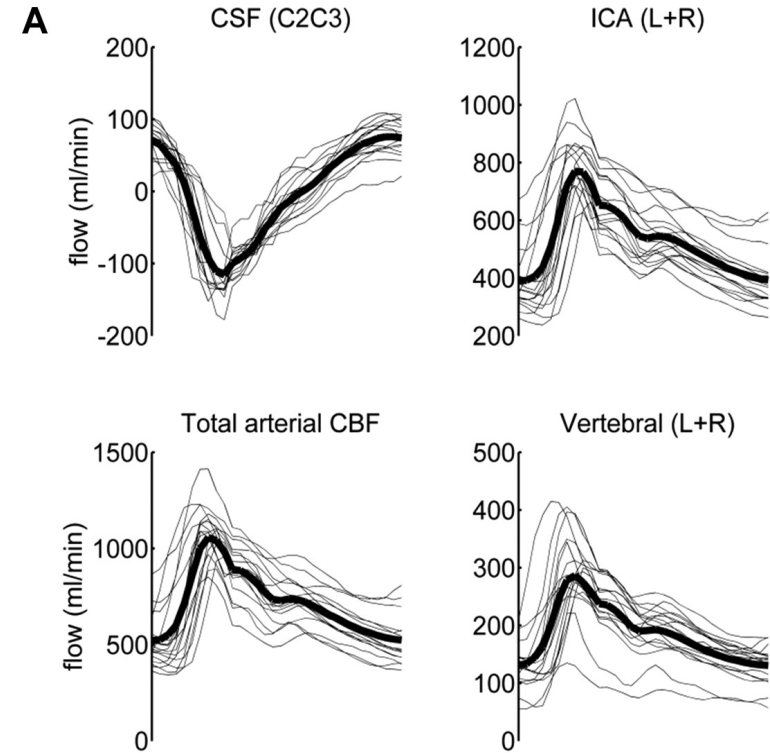
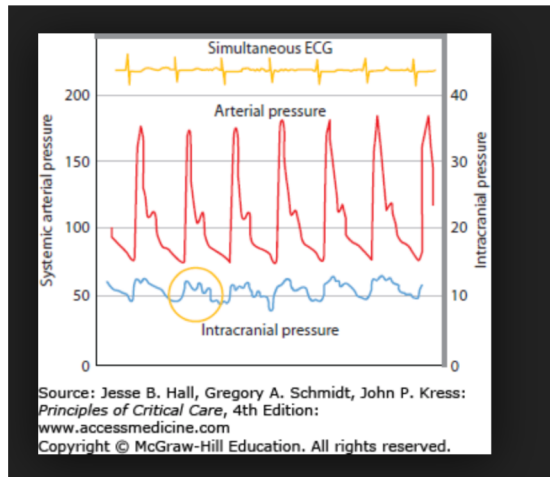
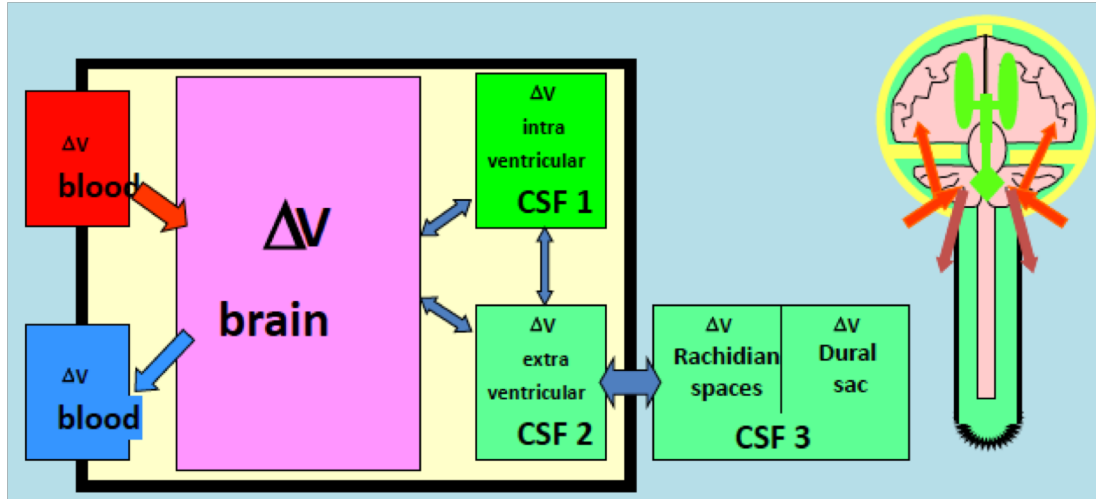


After a considerable amount of investigation on iNPH, it remains unresolved the questions of why while the intracranial pressure (ICP) remains normal, the ventricles continue dilating despite free communication between the ventricles and the subarachnoid space.

# Specific Aims of our Study

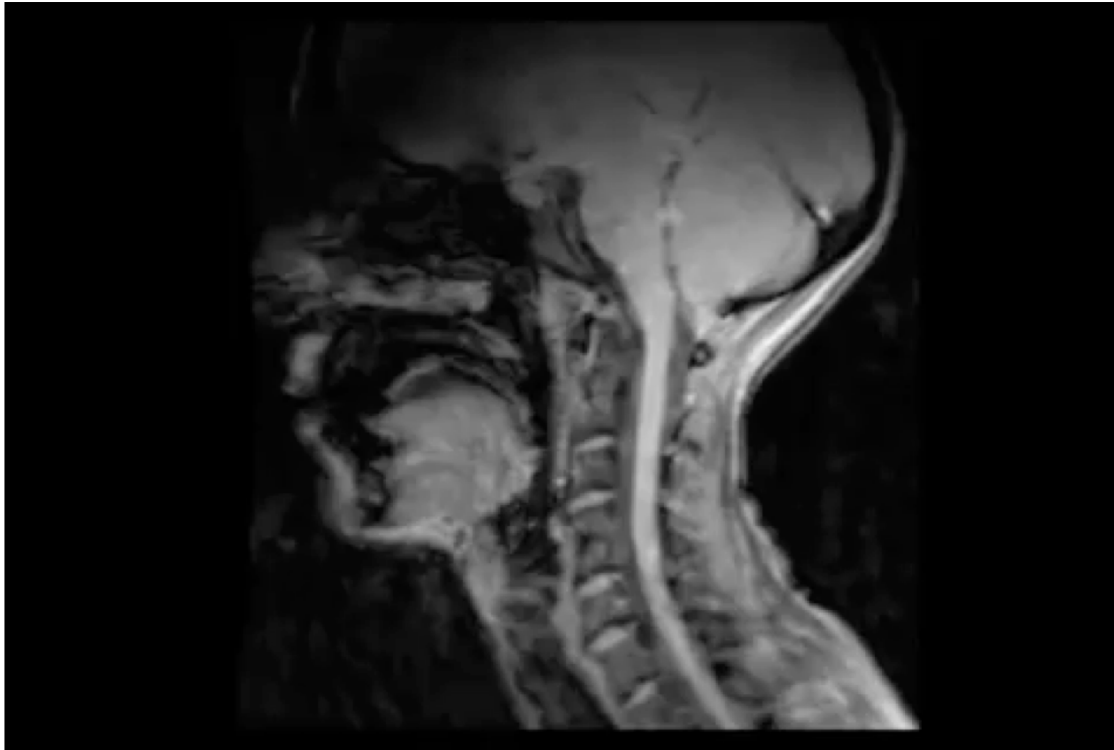
- To investigate the physical mechanism involved in the chronic ventricular enlargement in communicating iNPH
- Investigate the hypothesis that gradual changes in the elasticity and/or permeability (porosity) of the periventricular white matter may lead to a slow gradual enlargement of the ventricles without an increase in the mean intracranial pressure (ICP).
- Investigate this hypothesis through a computational model that incorporates recent MRE measurements of the changes in the viscoelastic properties of the brain tissue elderly population and in patients with iNPH.

# Some relevant considerations: 1



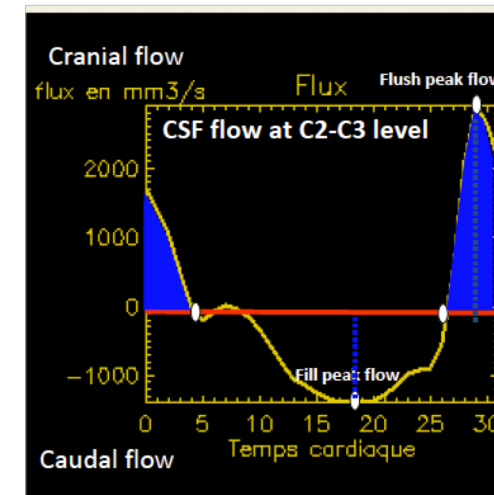
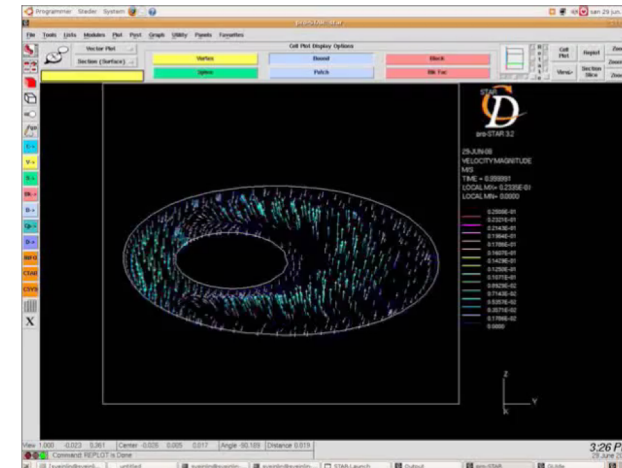
Compliant spinal canal      $\Delta V = 1-2 \text{ ml}$  ( $\Delta V = 2\%-3\%$ )  
 The systolic CSF inflow into the spinal SAS is accommodated by displacement of venous blood and/or the compression of fatty epidural tissue

## Some relevant considerations: 2

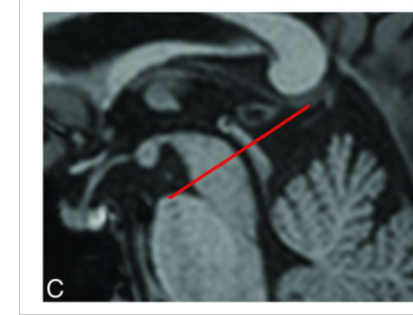
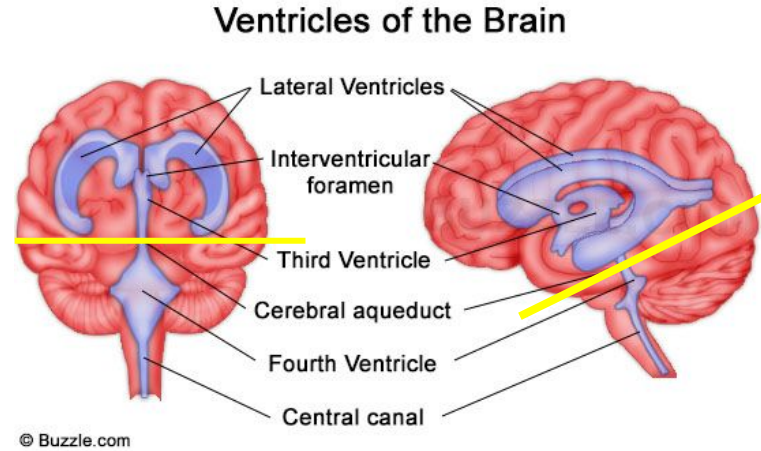


The spinal CSF fluctuates in biphasic tides of cephalic ebb and caudal flow. 1-2 mL of CSF (2%-3% of the total volume in the spinal canal) are displaced in and out of the cervical SAS during each cardiac cycle.

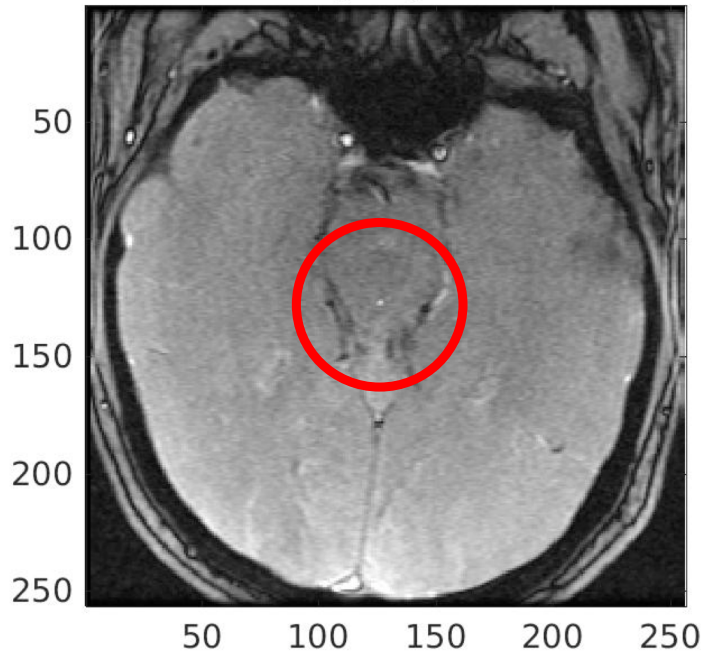
$$\Delta V/V \sim 0.02 - -0.03$$



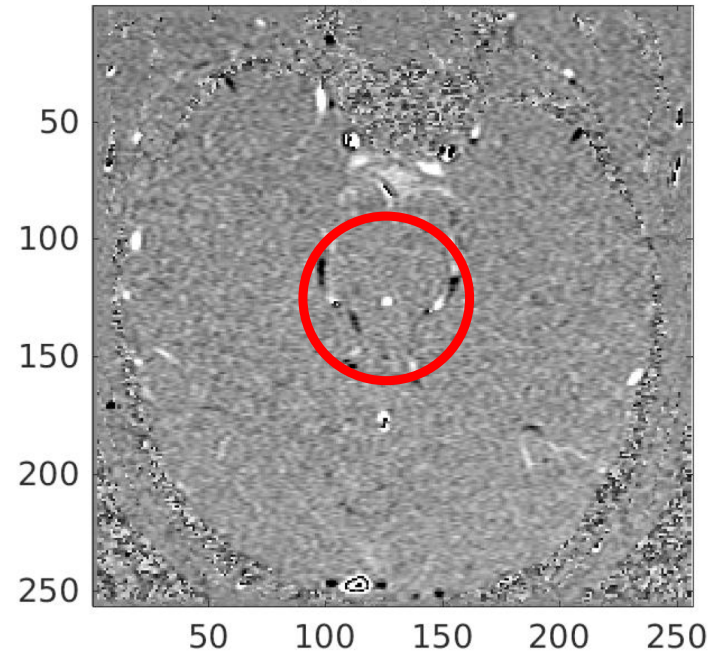
# Some relevant considerations: Oscillatory Flow of the CSF in the Cerebral Aqueduct



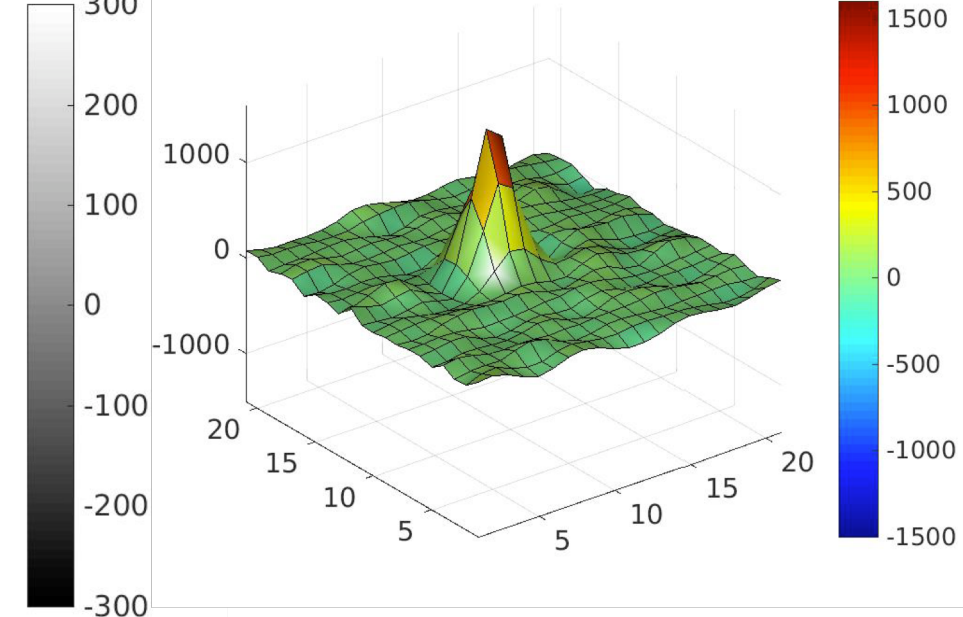
Anatomy equ.  $i = 31$



Velocity equ.  $i = 1$

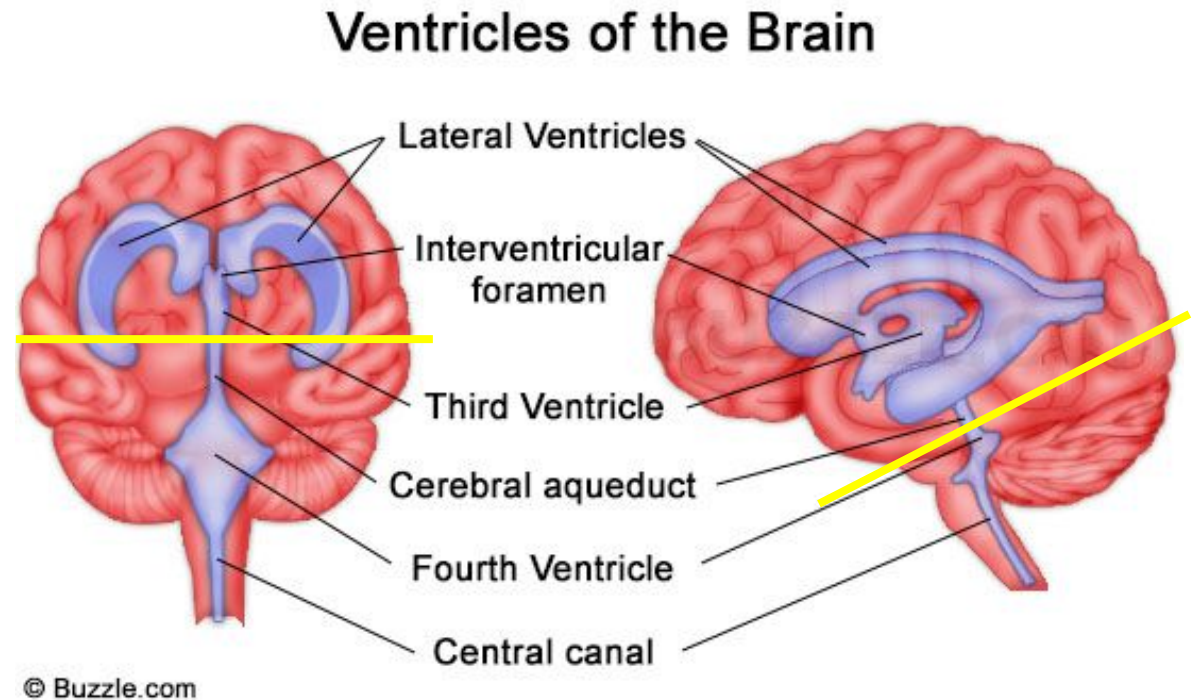
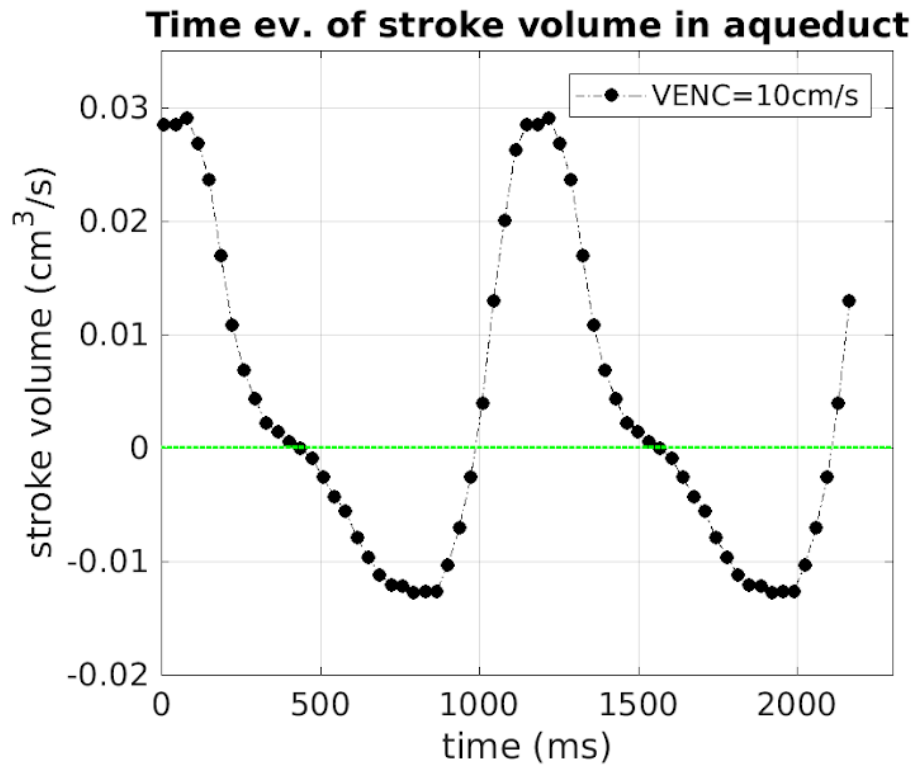


Aqueduct.  $i = 1$





# The volume of the ventricles increase and decrease with the oscillations of the stroke volume of CSF in the Cerebral Aqueduct



CSF normally flows back and forth through the aqueduct during the cardiac cycle. During systole, the brain and intracranial vasculature expand increasing the pressure in the lateral and third ventricles, forcing CSF craniocaudal. During diastole, the pressure in the ventricle decreases and flow through the aqueduct reverses.

## MRI observations of the volume oscillations of the ventricles are consistent with the oscillations of the stroke volume of CSF we measure in the Cerebral Aqueduct

*Variation of Lateral Ventricular Volume During the Cardiac Cycle Observed by MR Imaging.* Ellen Lee, Jin-zhao Wang, Reuben Mezrich. *AJNR* 10:1145-1149, 1989

In 12 normal individuals, the cerebral ventricles were examined, and the size of the lateral ventricles showed a **10-20% change** during the cardiac cycle. The temporal variation was consistent for all the individuals.

The pattern is complex but similar in appearance to the intracranial pressure pulse waveform

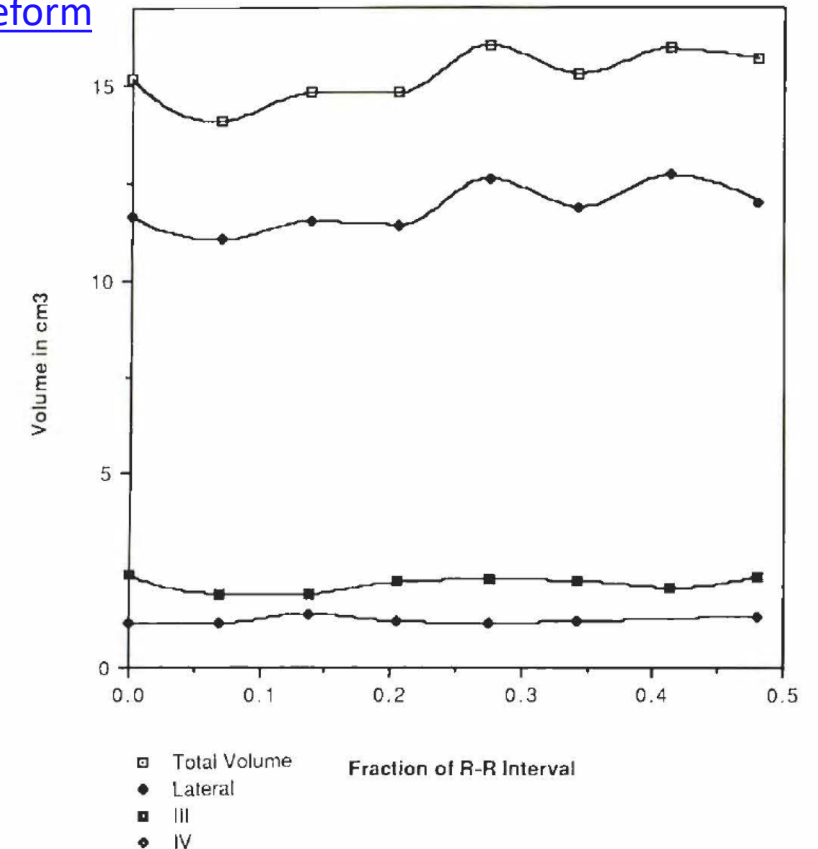
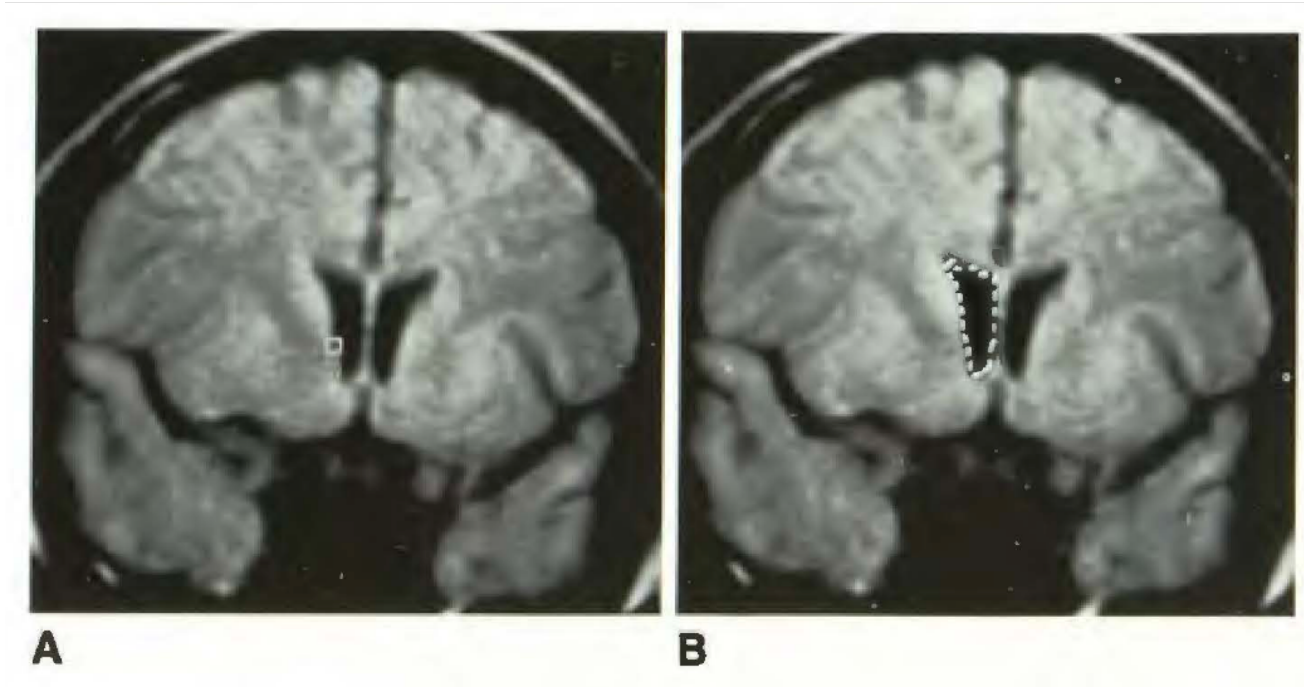


Fig. 6.—Gated total, lateral, third, and fourth ventricular volumes. The curves of the total and lateral ventricles are similar. The curves of the third and fourth ventricles are relatively flat.

This suggests that the Choroid Plexuses play a greater role in the CSF pulsations than previously suggested

# Transmural Pressure calculated from measurements of the time variation of the CSF velocity in the cerebral aqueduct

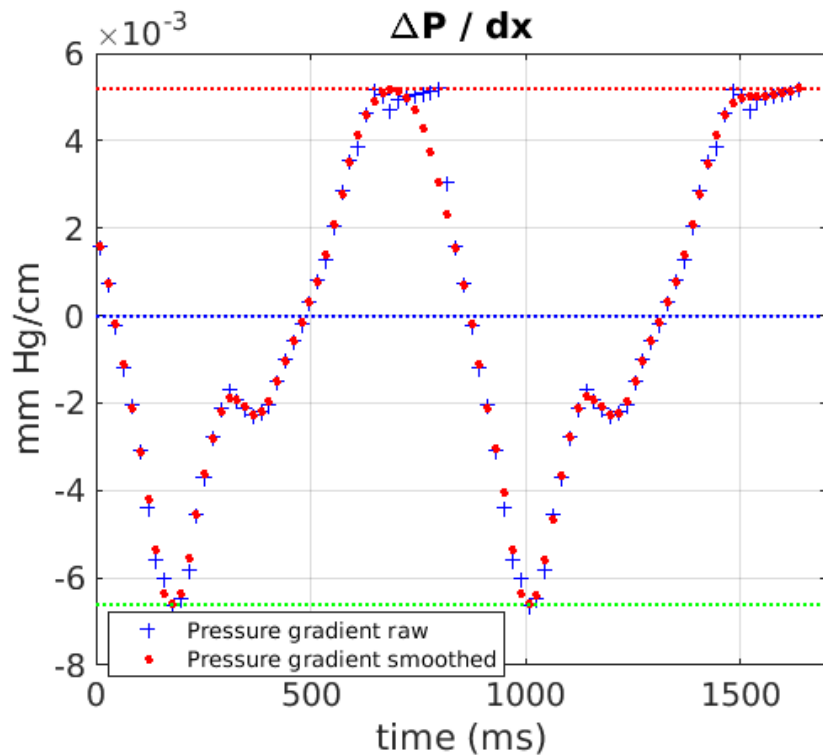
incompressible Navier-Stokes equations

$$\nabla \cdot \vec{V} = 0$$

$$\rho \frac{\partial \vec{V}}{\partial t} + \rho (\vec{V} \cdot \nabla) \vec{V} = -\nabla p + \mu \nabla^2 \vec{V} + \rho \vec{g}$$

X-momentum

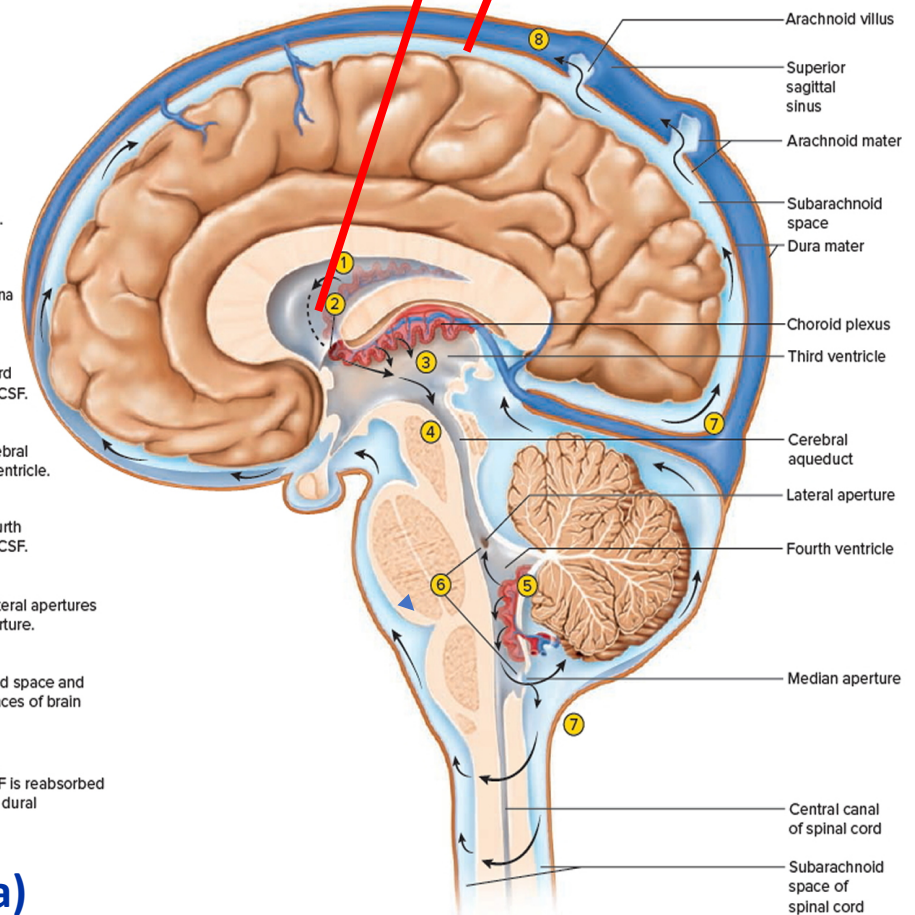
$$\rho \left( \frac{\partial U}{\partial t} + U \frac{\partial U}{\partial x} + V \frac{\partial U}{\partial y} + W \frac{\partial U}{\partial z} \right) = -\frac{\partial P}{\partial x} + \rho g_x + \mu \left( \frac{\partial^2 U}{\partial x^2} + \frac{\partial^2 U}{\partial y^2} + \frac{\partial^2 U}{\partial z^2} \right)$$

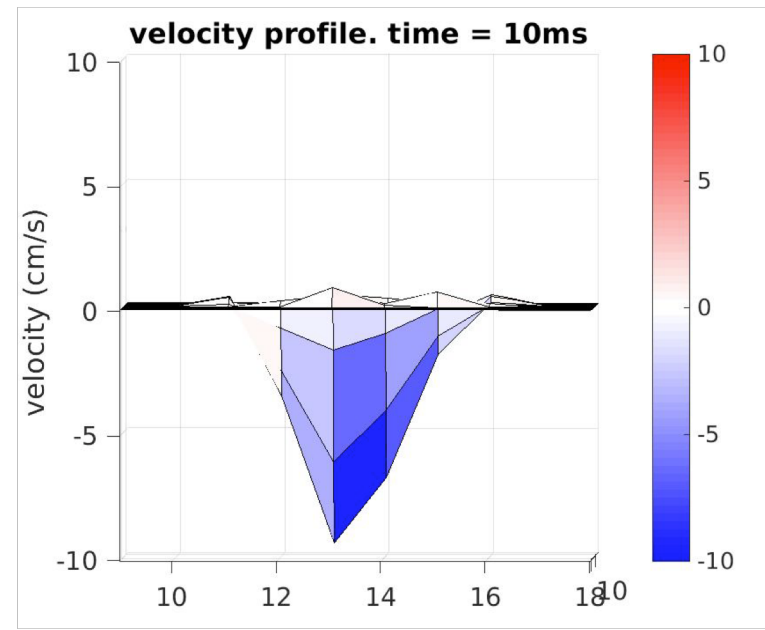
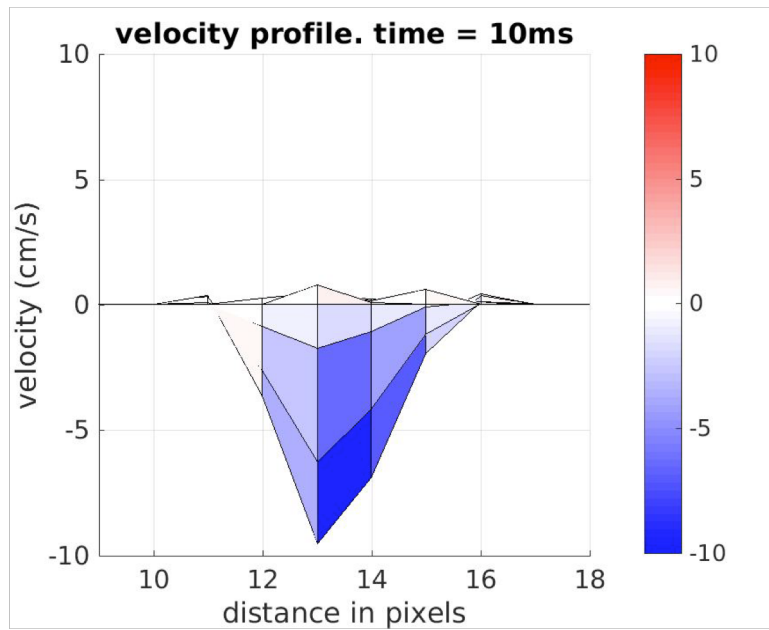
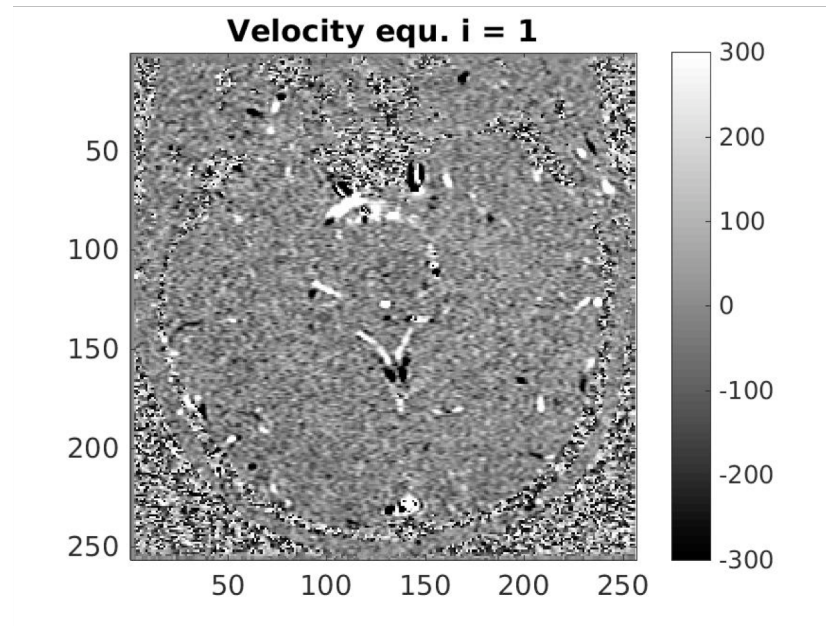


Transmantle pressure  $\Delta P_t = P_v - P_{SAS} = 0.09 - 0.14 \text{ mmHg} (100 - 200 \text{ Pa})$

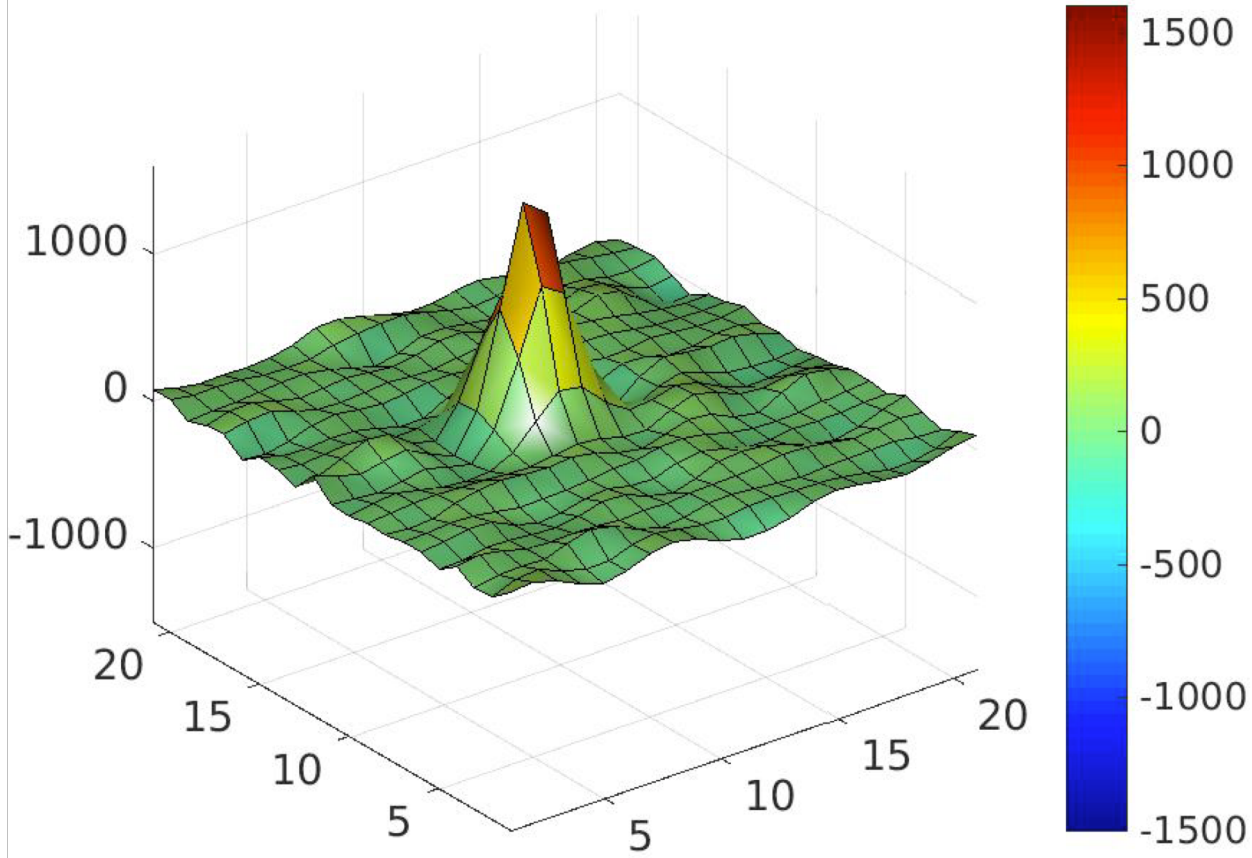
Transmantle pressure  $P_t = P_v - P_{SAS}$

- 1 CSF is secreted by choroid plexus in each lateral ventricle.
- 2 CSF flows through interventricular foramina into third ventricle.
- 3 Choroid plexus in third ventricle adds more CSF.
- 4 CSF flows down cerebral aqueduct to fourth ventricle.
- 5 Choroid plexus in fourth ventricle adds more CSF.
- 6 CSF flows out two lateral apertures and one median aperture.
- 7 CSF fills subarachnoid space and bathes external surfaces of brain and spinal cord.
- 8 At arachnoid villi, CSF is reabsorbed into venous blood of dural venous sinuses.

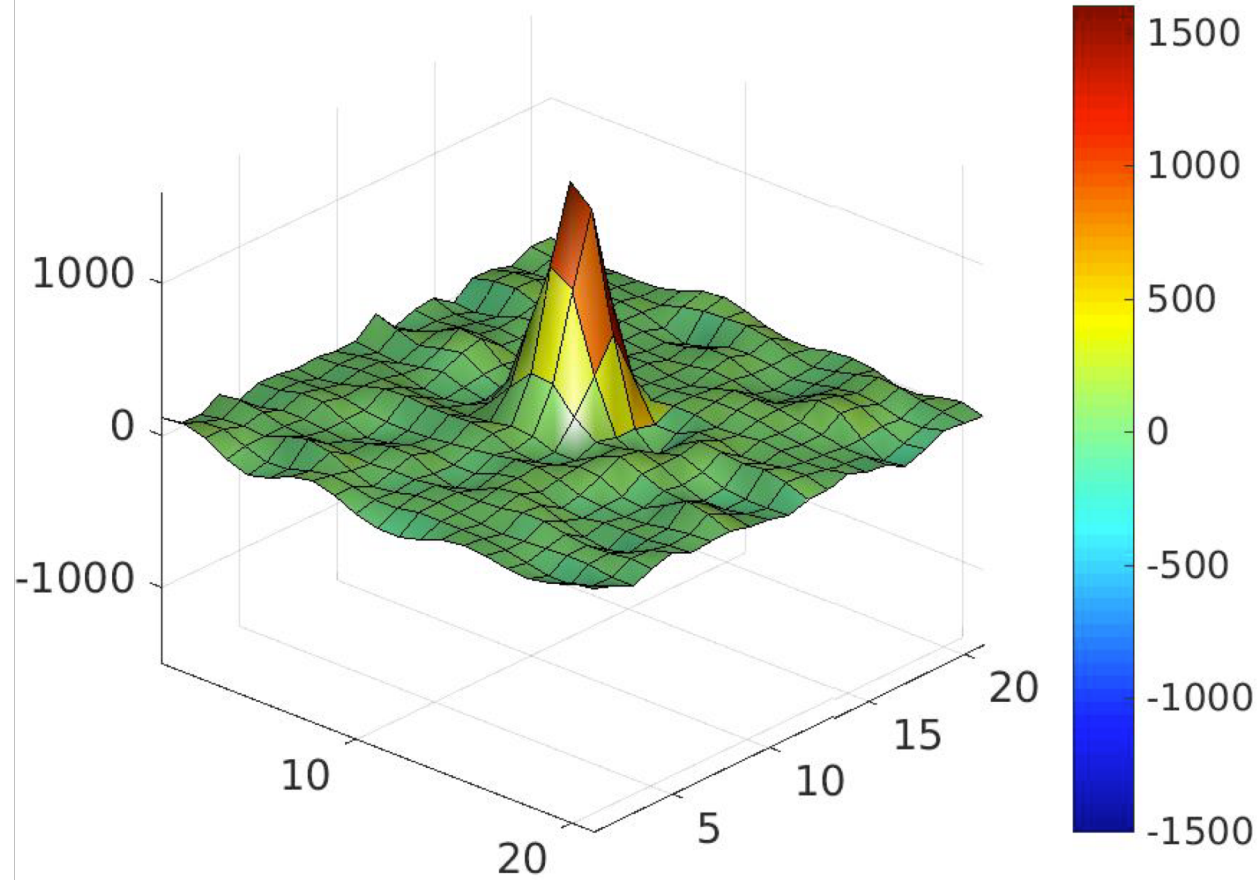




**Aqueduct. i = 1**

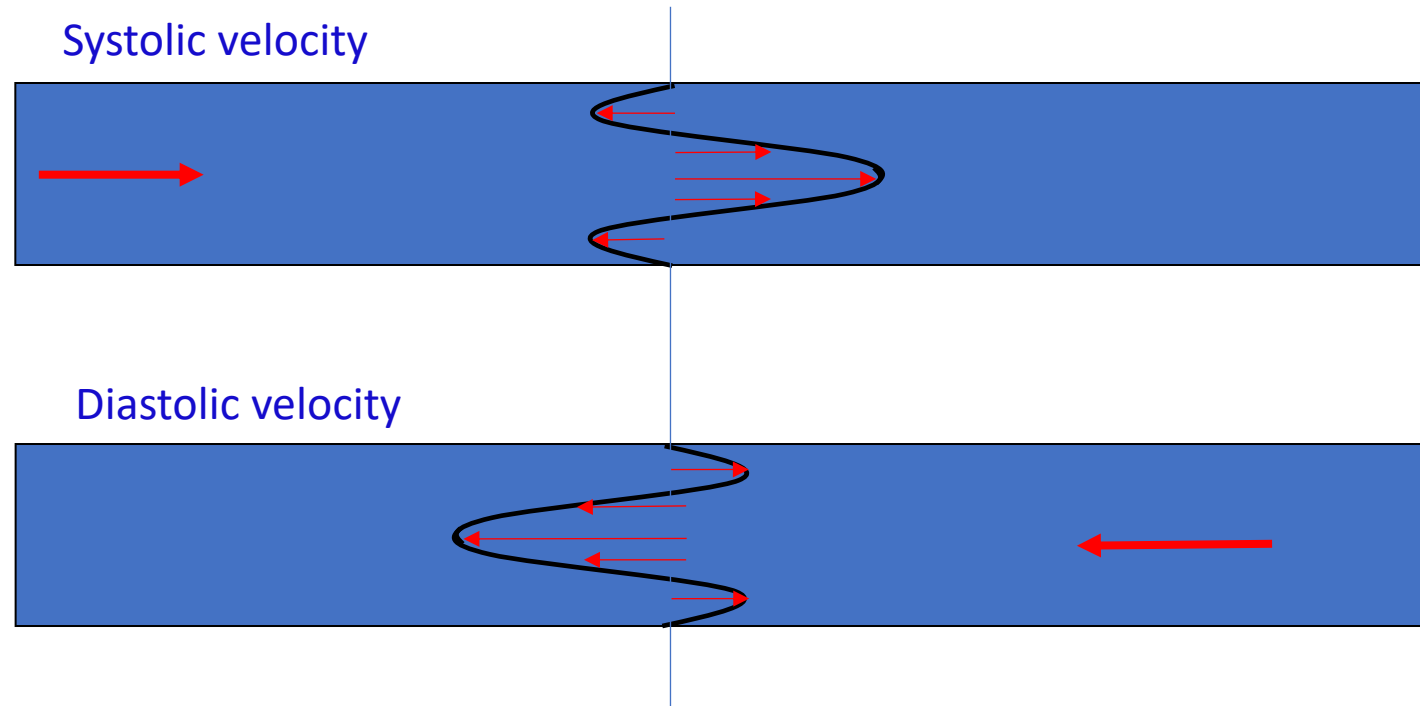


**Aqueduct. i = 1**



# Womersley Flow. Oscillatory flow in a pipe

$$\underbrace{\frac{\partial \mathbf{v}}{\partial t}}_{\text{inertia}} + \mathbf{v} \cdot \nabla \mathbf{v} = -\nabla \left( \frac{p}{\rho} \right) + \underbrace{\nu \nabla^2 \mathbf{v}}_{\text{viscosity}} \quad \frac{\mathcal{O}(\partial \mathbf{v} / \partial t)}{\mathcal{O}(\nu \nabla^2 \mathbf{v})} \sim \alpha^2 = \left( \frac{h_c}{\nu / \omega} \right)^2 \quad \text{Womersley number}$$



Circular tube under a periodic pressure gradient. Womersley (1954)

A.-V. Salsac, S. R. Sparks, J.-M. Chomaz and J. C. Lasheras. J. Fluid Mech. (2006)

Circular tube under a periodic pressure gradient. Womersley (1954)

A.-V. Salsac, S. R. Sparks, J.-M. Chomaz and J. C. Lasheras. J. Fluid Mech. (2006)

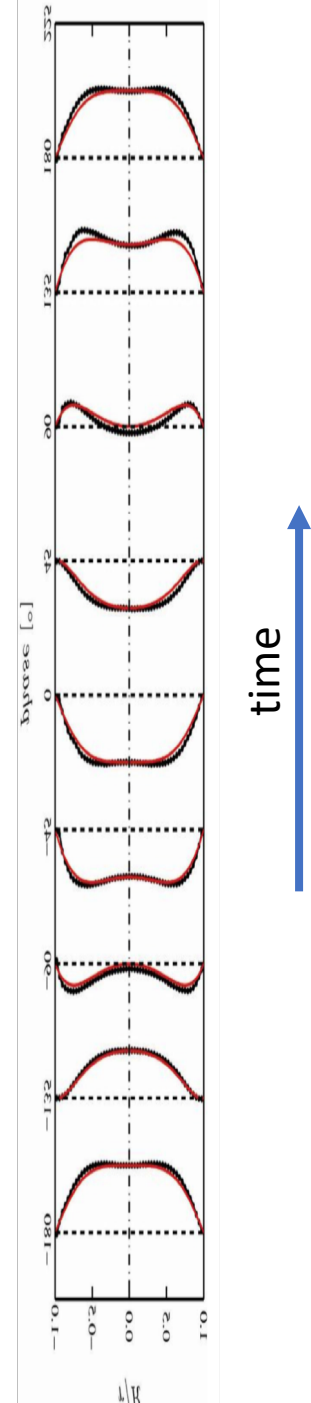
$$v^*(r^*, t^*) = \frac{ReG_0^*}{4}(1 - r^{*2}) + \frac{Re}{i} \sum_{n=1}^{\infty} \frac{G_n^*}{\alpha_n^2} \left( 1 - \frac{J_0(r^* i^{3/2} \alpha_n)}{J_0(i^{3/2} \alpha_n)} \right) e^{int^*}$$

$$G_0^* = \frac{8}{\pi Re} Q_0^*; \quad G_n^* = \frac{i \alpha_n * 2}{Re(1 - F(\alpha_n))} Q_n^*,$$

$$F(\alpha_n) = \frac{2}{i^{3/2} \alpha_n} \frac{J_1(i^{3/2} \alpha_n)}{J_0(i^{3/2} \alpha_n)}.$$

X-momentum

$$\rho \left( \frac{\partial U}{\partial t} + U \frac{\partial U}{\partial x} + V \frac{\partial U}{\partial y} + W \frac{\partial U}{\partial z} \right) = -\frac{\partial P}{\partial x} + \rho g_x + \mu \left( \frac{\partial^2 U}{\partial x^2} + \frac{\partial^2 U}{\partial y^2} + \frac{\partial^2 U}{\partial z^2} \right)$$



# Transmantle pressure increases as the volume of the ventricles increases

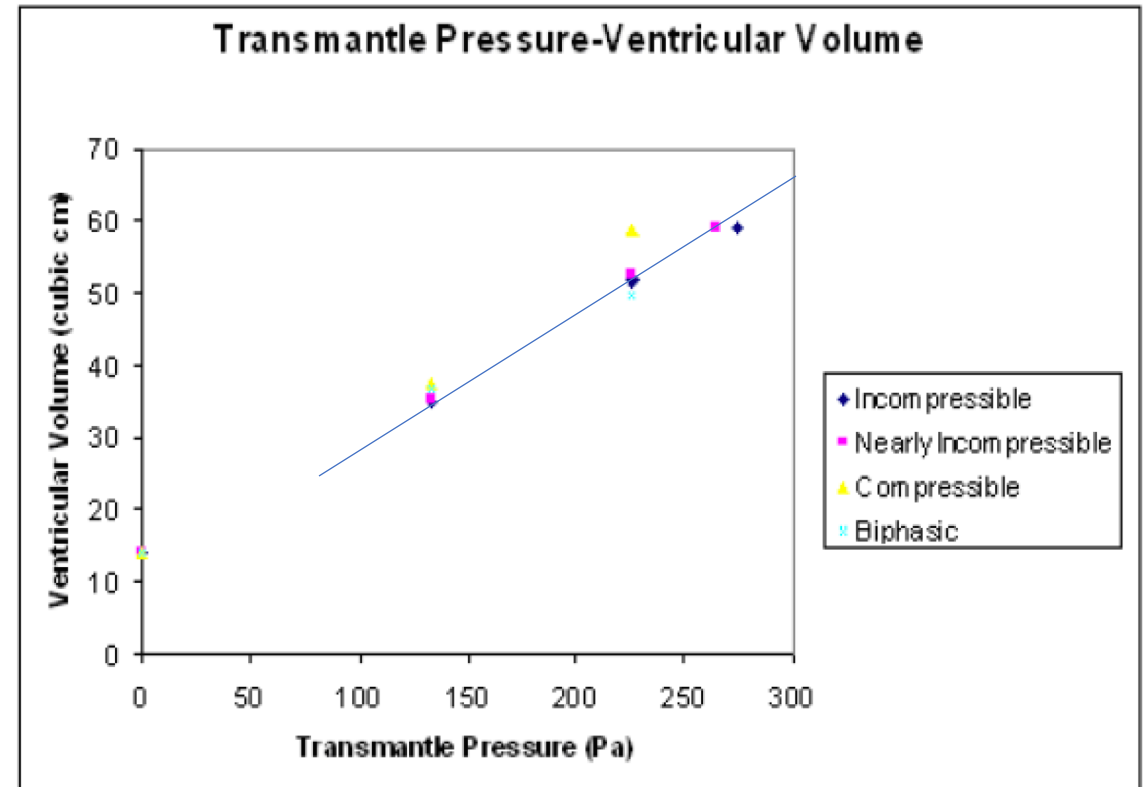
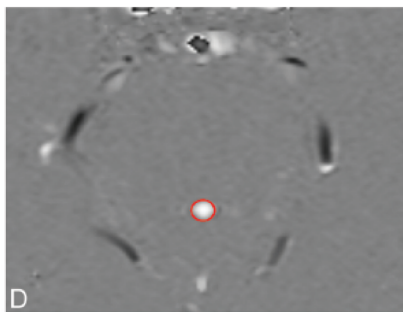
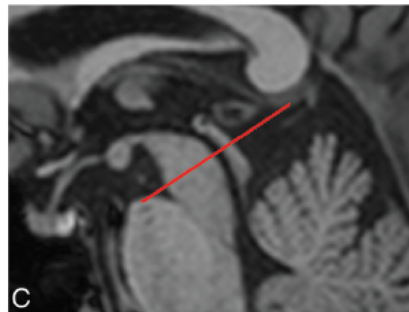
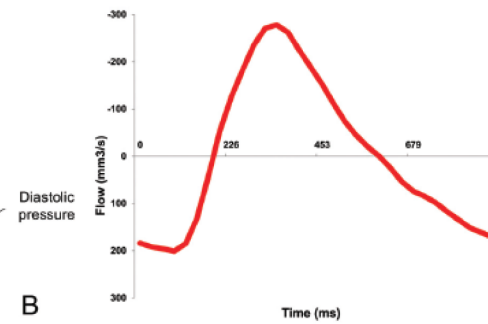
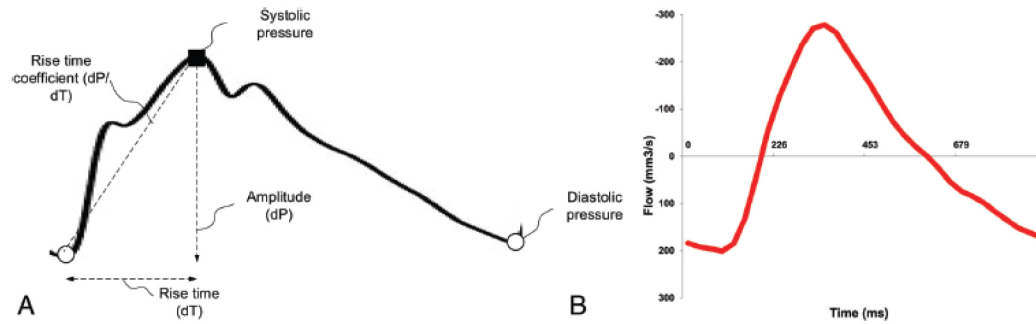
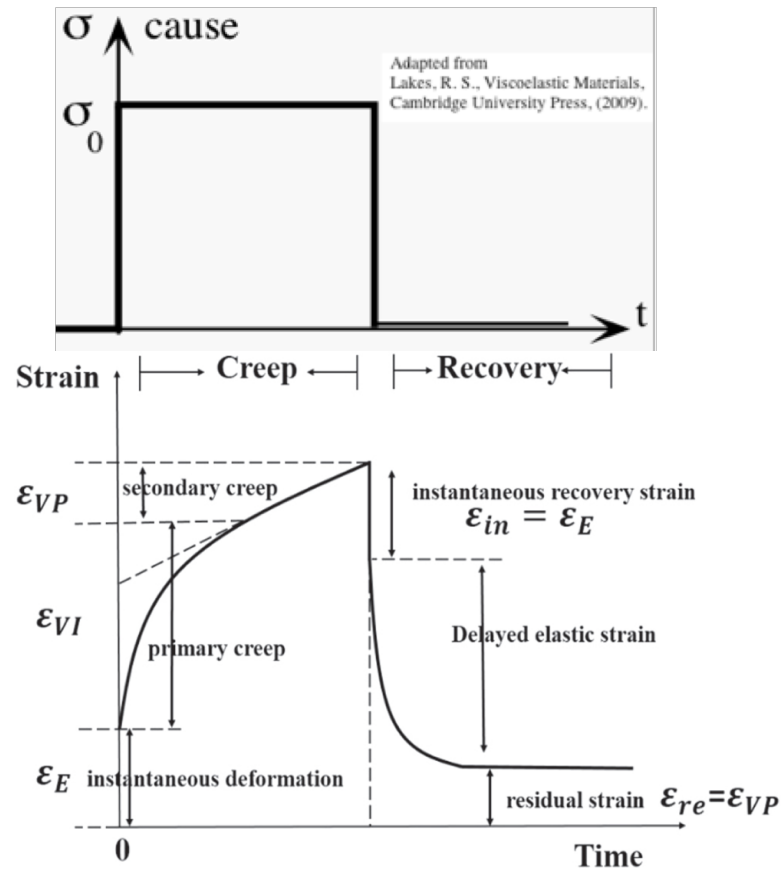
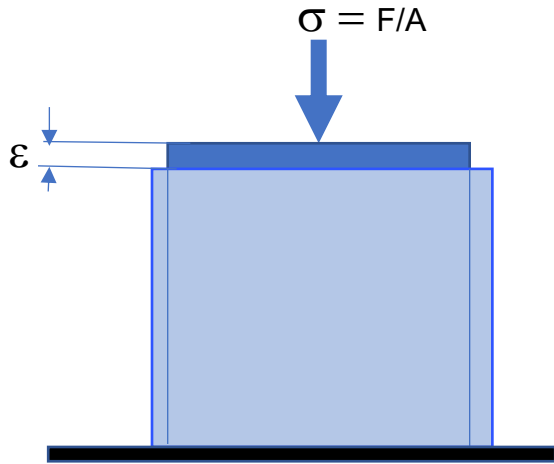


**Figure 3.2:** Transmantle pressure difference v/s ventricular volume for single phase (incompressible, nearly incompressible and compressible) and biphasic brain model

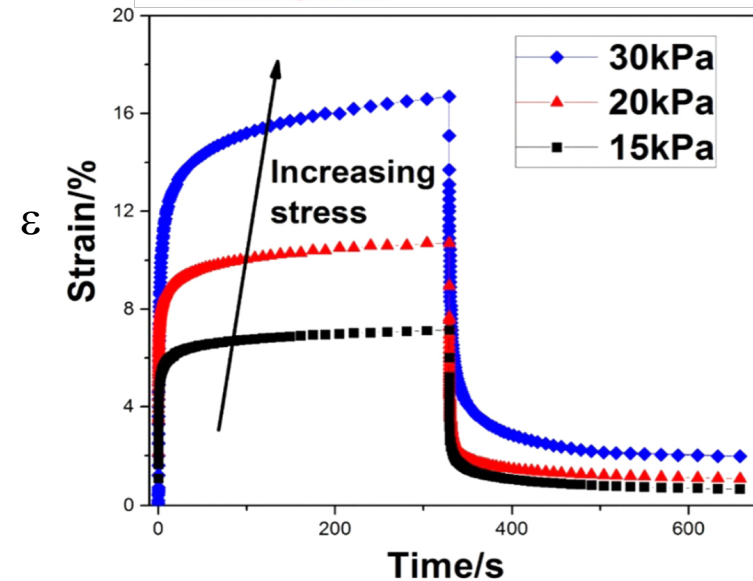
# Some additional relevant considerations

Brain is a elastic porous media with interstitial fluid that exhibits creep and recovery and can be modeled as a viscoelastic material

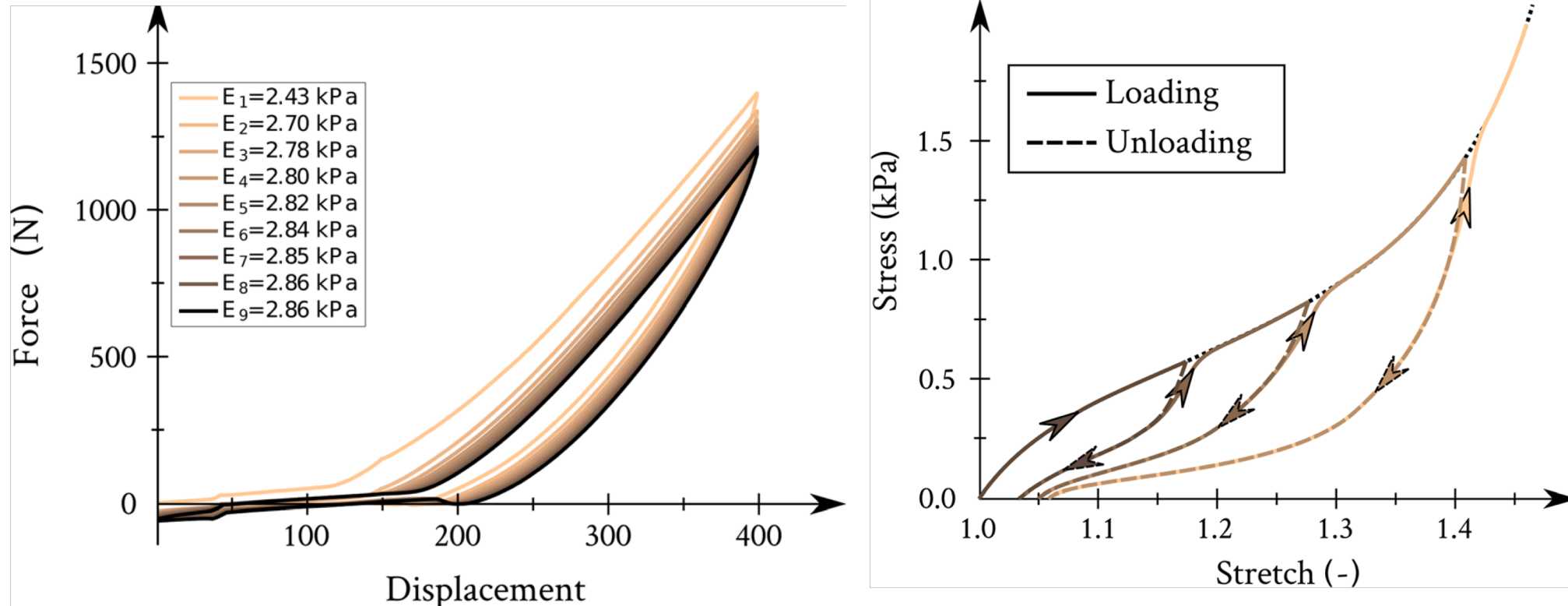


properties of the brain similar to other viscoelastic materials

- :
- hysteresis is seen in the stress-strain curve
- stress relaxation occurs: **step constant strain causes decreasing stress**
- creep occurs: **step constant stress causes increasing strain**



# Hysteresis of the Brain Parenchyma



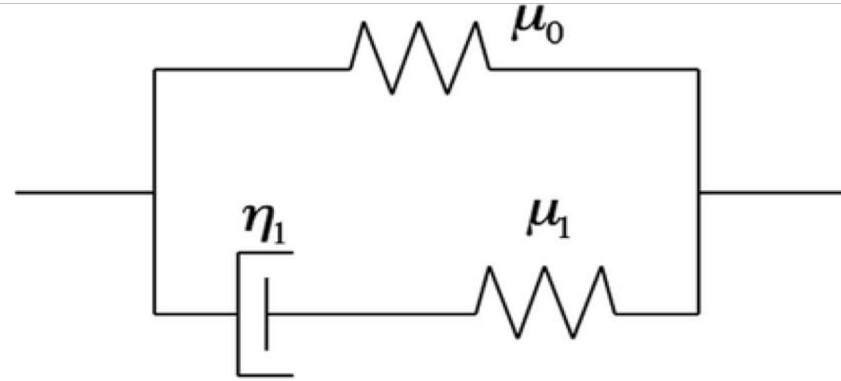
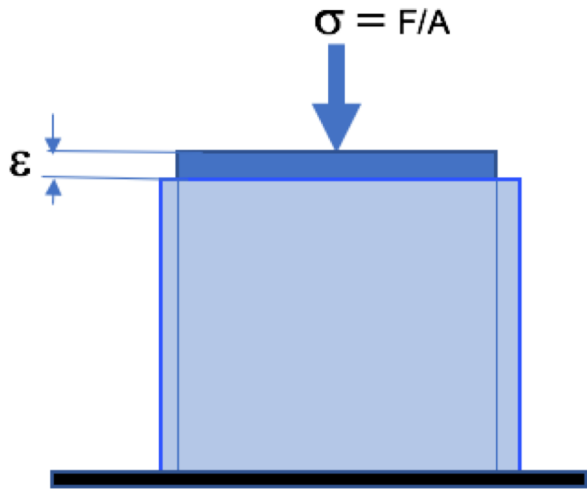
History-dependent response of the brain tissue under uniaxial loading–unloading.

[Constitutive Modeling of Brain Tissue: Current Perspectives](#)

Rijk de Rooij and Ellen Kuhl. *Appl. Mech. Rev.* 2016;68

Some relevant considerations : **Recovery time increases when the elasticity  $\mu$  of the brain decreases**

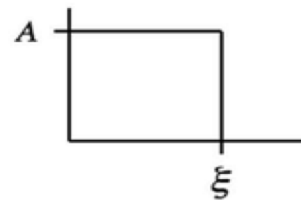
Standard linear solid (SLS) model  
(Zener model)



(a)

$$F(t) = A[U(t) - U(t - \xi)] \rightarrow \frac{\tau_\epsilon}{E_\mu \tau_\sigma} \delta(t) + \frac{(\tau_\sigma - \tau_\epsilon)}{E_\mu \tau_\sigma^2} e^{-\frac{t}{\tau_\sigma}} \rightarrow x(t) = \begin{cases} \frac{A}{E_\mu} - \frac{A(\tau_\sigma - \tau_\epsilon)}{E_\mu \tau_\sigma} e^{-\frac{t}{\tau_\sigma}}; & \text{for } 0 < t < \xi \\ \frac{A(\tau_\sigma - \tau_\epsilon)}{E_\mu \tau_\sigma} \left( e^{\frac{\xi}{\tau_\sigma}} - 1 \right) e^{-\frac{(t-\xi)}{\tau_\sigma}}; & \text{for } t > \xi \end{cases}$$

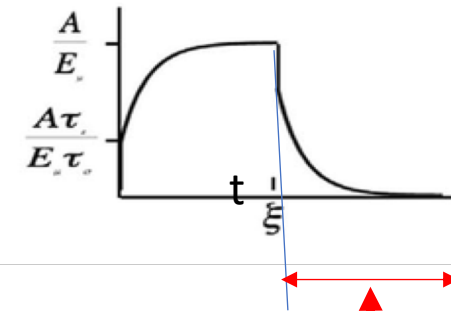
(b)



\*

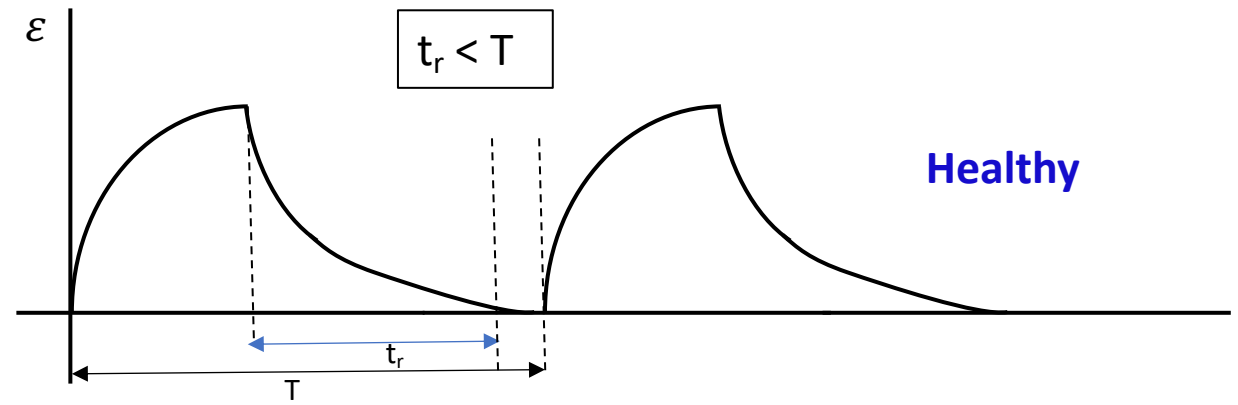
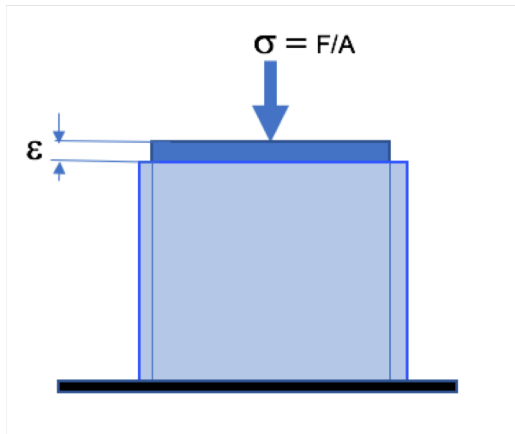
Impulse Response

=

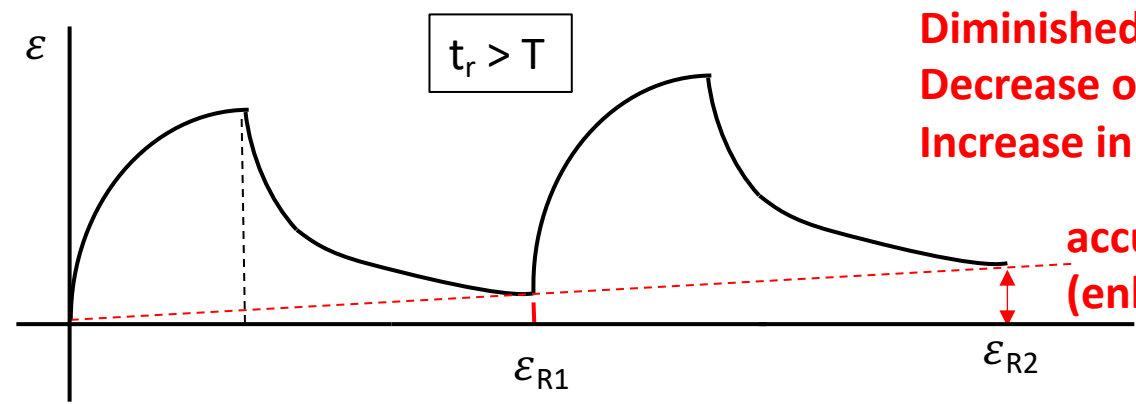


$t_r$  = Recovery (Relaxation) Time proportional to  $\eta_1/\mu_1$   
 $\mu_1$  = stiffness ;  $\eta_1$  = inverse of the permeability ( $\alpha$ )

**Hypothesis:** Response under the cyclic loading of transmural pressure may lead to an increase in the recovery time and a gradual accumulation of strain (enlargement of the ventricles) when the elasticity of the WM and/or the permeability decreases, and/or the transmante pressure increase, while the mean ICP remains constant



Healthy



Diminished Brain Elasticity  
Decrease of Permeability  
Increase in the Transmante Pressure

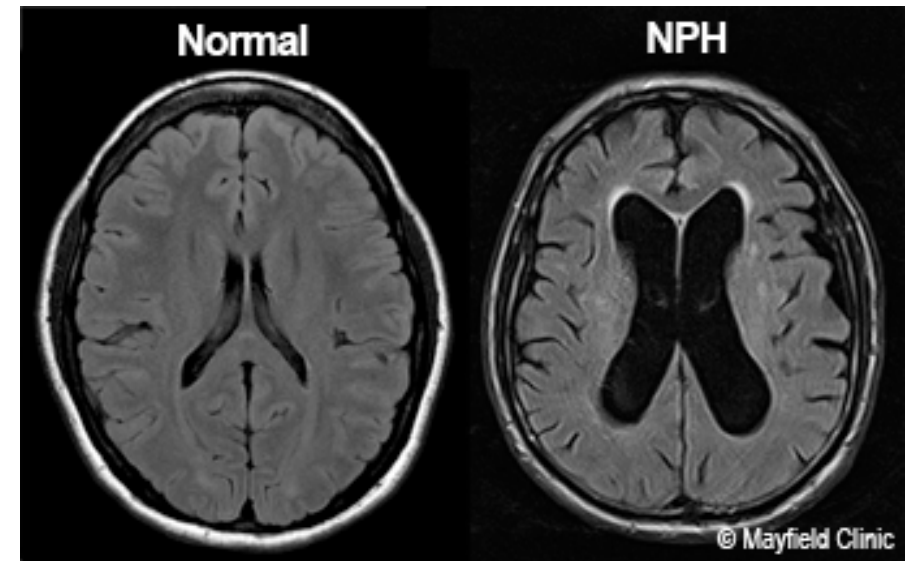
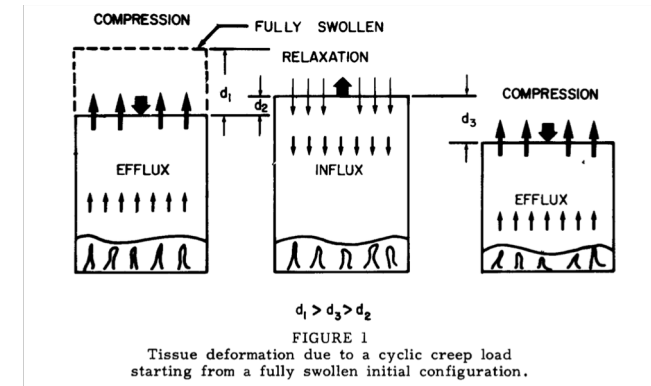
accumulation of strain  
(enlargement of the ventricles)

# How large needs to be the residual (accumulation ) strain per cycle to result in iNPH?

The iNPH progresses insidiously over long periods of time, presumably over several months, or even years.

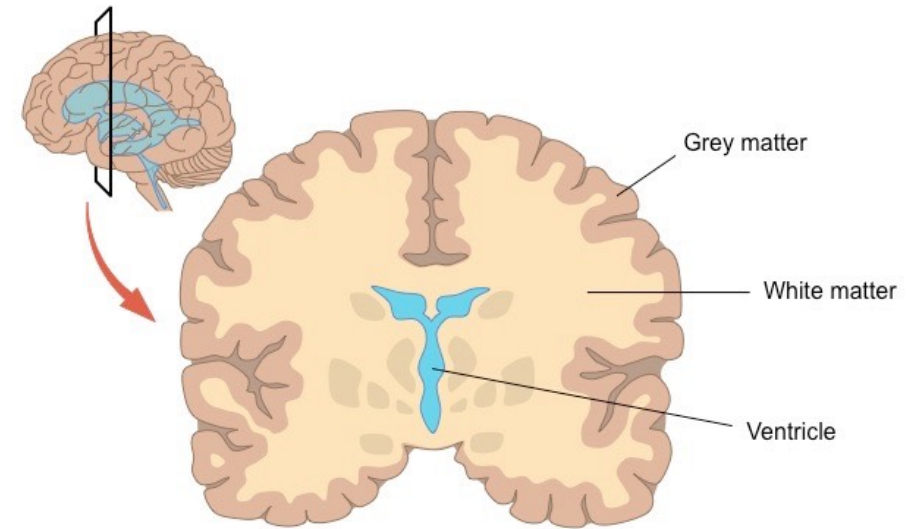
Let us assume conservatively that it has developed over a 6 month period = 15,768,000 cardiac cycles. A residual strain  $\epsilon$  of  $0.01 \mu\text{m} = 1/100,000 \text{ mm}$  per cycle will result after 6 months in a permanent residual strain (enlargement of the ventricle) of **1.57 cm**

.... or **3 cm** in one year (31,556,952 cardiac cycles)

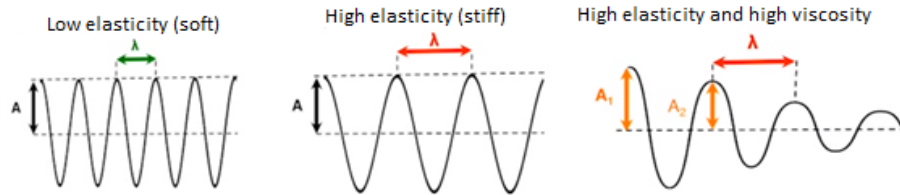
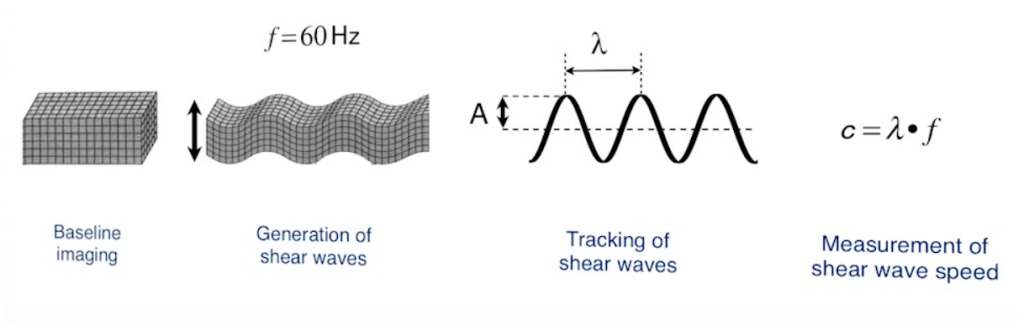


What do we know about the Viscoelastic properties of the brain in iNPH patients?

In particular, what do we know about the elasticity ( $m$ ) and/or permeability (porosity) ( $a$ ) of the periventricular white matter (WM) in these patients?



# Measurement of Brain Viscoelastic Properties using MRE



- Transmit shear waves to head via passive drive:
  - Bite-bar
  - Head cradle
  - Soft pillow
- Actuation frequency: 10-100 Hz
- Tissue displacement is determined by measuring wavelength to infer inherent material property
- Displacement is transformed into stiffness maps or *elastograms*

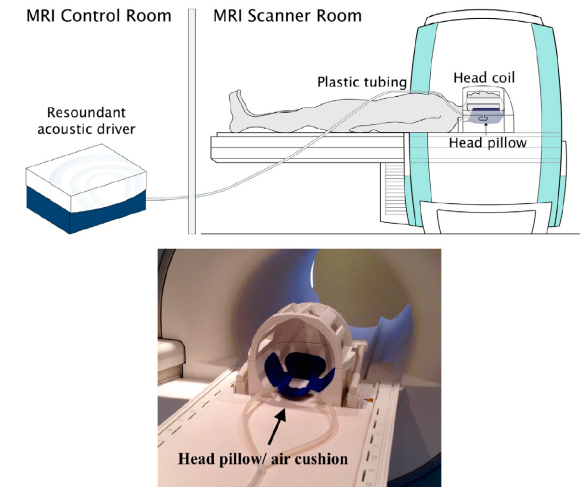
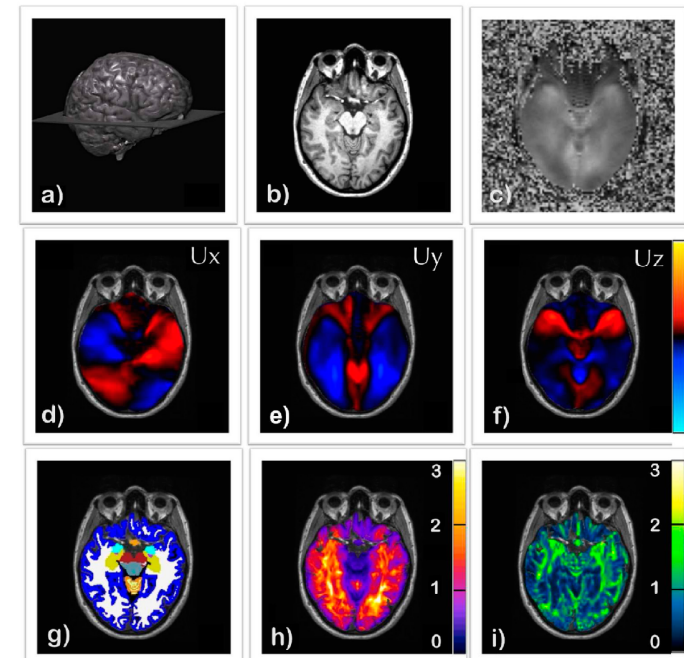


Figure 2. (a) Schematic diagram of the pneumatic actuator with head-pillow driver (Resonant, Mayo Clinic, Rochester, MN, USA), (b) Photograph of the head-pillow within the MRI head-coil.



# Calculating tissue mechanical properties

- Viscoelastic tissue properties determined by calculating complex shear modulus  $G^*$  written as:

$$G^* = G' + iG''$$

$G'$  = Shear storage Modulus. Measures of mechanical energy stored

$G''$  = Shear Loss Modulus. Measures the energy dissipated represented by wave attenuation (i.e. greater loss in amplitude = greater material viscosity)

- Magnitude  $|G^*| = (G'^2 + G''^2)^{1/2}$  - most similar to the information afforded by manual palpation includes both elasticity and viscosity
- Loss tangent:  $\varphi = \arctan (G''/G')$  – for relative tissue viscosity
- Shear stiffness:

$$G_s = \rho v_s^2 = \frac{2(G'^2 + G''^2)}{G' + \sqrt{(G'^2 + G''^2)}}$$

# Viscoelastic Model of the Brain Parenchyma

Additional processing- multi-frequency MRE

The model-dependent viscoelastic parameters are determined by minimizing the error:

$$\chi = \frac{1}{N} \sum_{n=1}^N \sqrt{(\text{Re}[G(\omega_n) - G_M(\omega_n)])^2 + (\text{Im}[G(\omega_n) - G_M(\omega_n)])^2},$$

where N denotes the number of driving frequencies

Based on these measurements the viscoelasticity of the brain parenchyma is best represented by the **Zener model (Standard Linear Model)** and/or the **Springpot model (Fractional Calculus model)**

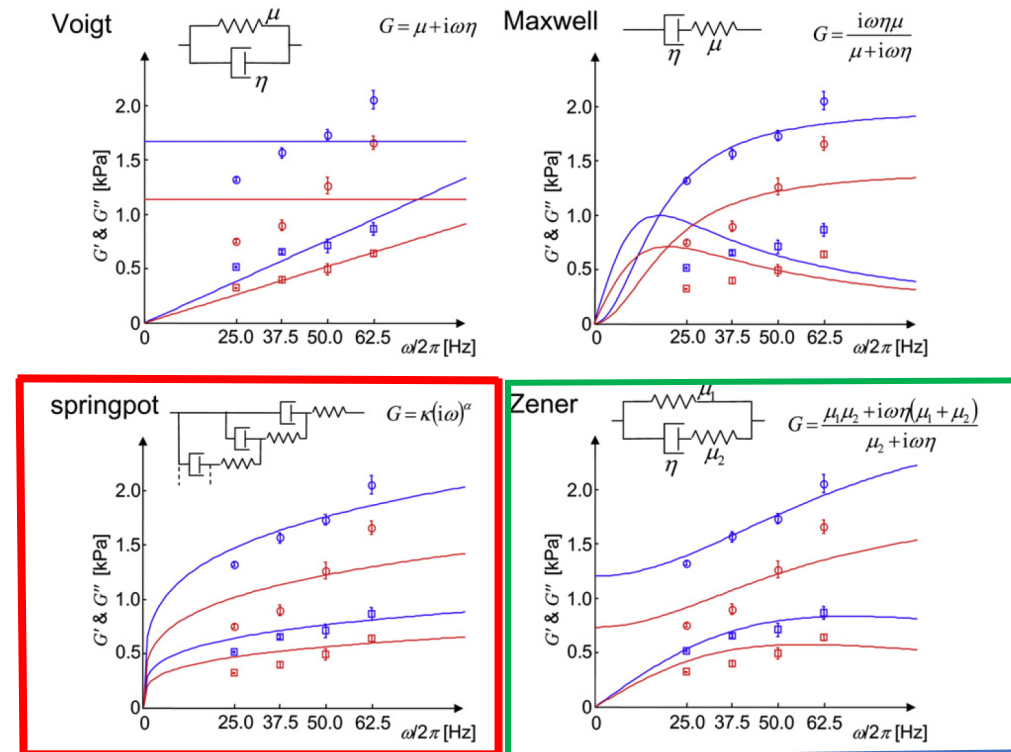


**Fig. 3.** Representations of the complex modulus  $G(\omega)$  as real and imaginary parts on a frequency axis (storage and loss modulus  $G'$  and  $G''$  are represented by circles and squares, respectively). Blue data correspond to the youngest volunteer (female, 18 years) while red data represent the oldest volunteer in our cohort (female, 88 years). Fits were performed according to the simplest (two-parameter) viscoelastic models and the Zener model. In addition, the spring-dashpot representations of all models together with the fit functions,  $G(\omega)$ , are given.

# Springpot Model

Springpot model ← fractional calculus

$$\sigma(t) = \mu^{1-\alpha} \eta^\alpha \frac{\partial^\alpha \epsilon}{\partial t^\alpha}$$

$\sigma$  = stress

$\eta$  = viscosity  $\equiv 3.7$  Pa (water)

$\epsilon$  = strain

Both  $K = \mu^{1-\alpha} \eta^\alpha$  and  $\alpha$  are frequency dependent.


if  $\alpha = 0$ :

$$\sigma = \mu \epsilon$$

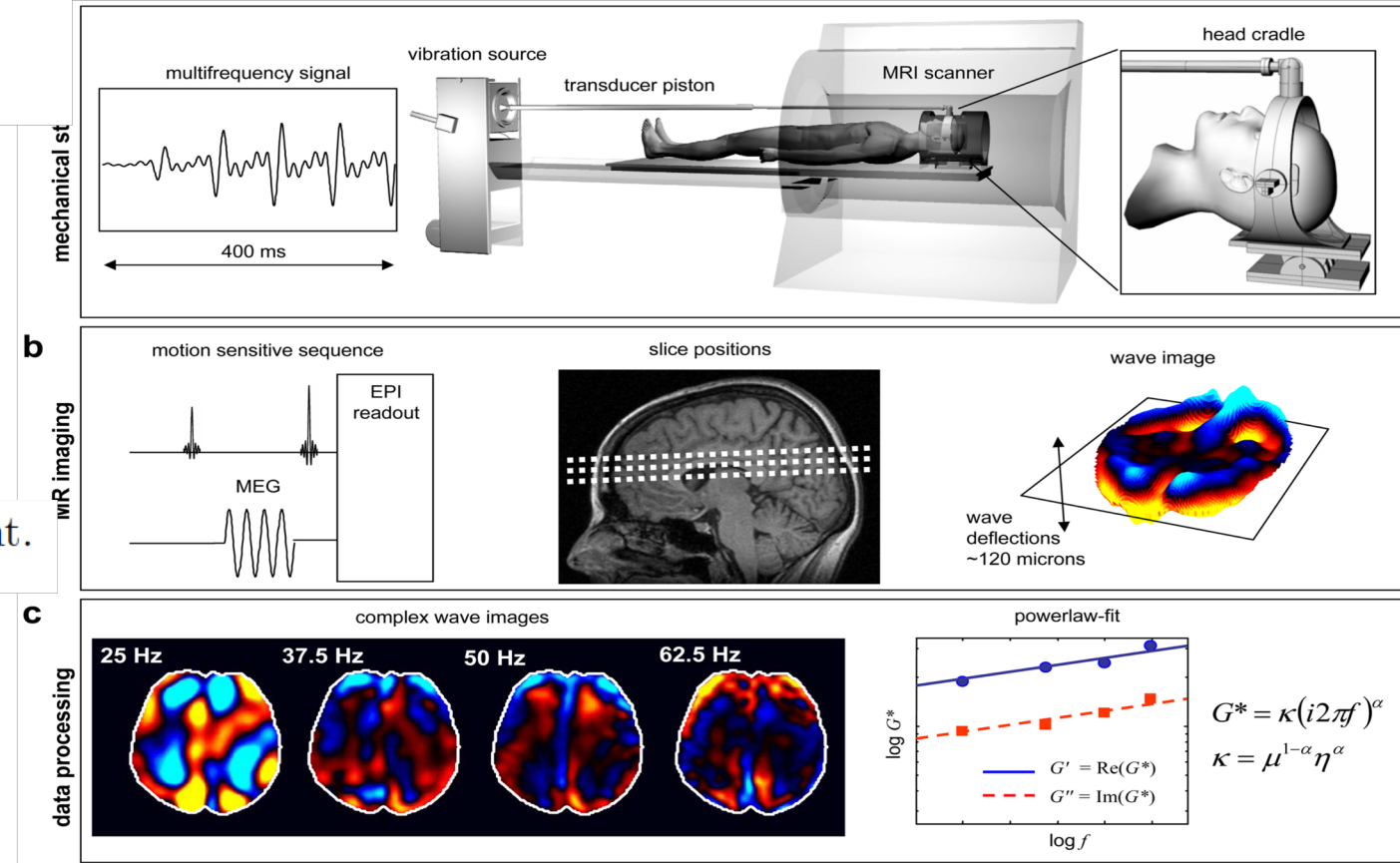
if  $\alpha = 1$ :

$$\sigma = \eta \frac{\partial \epsilon}{\partial t}$$

spring: 

dashpot: 

$$0 \leq \alpha \leq 1$$



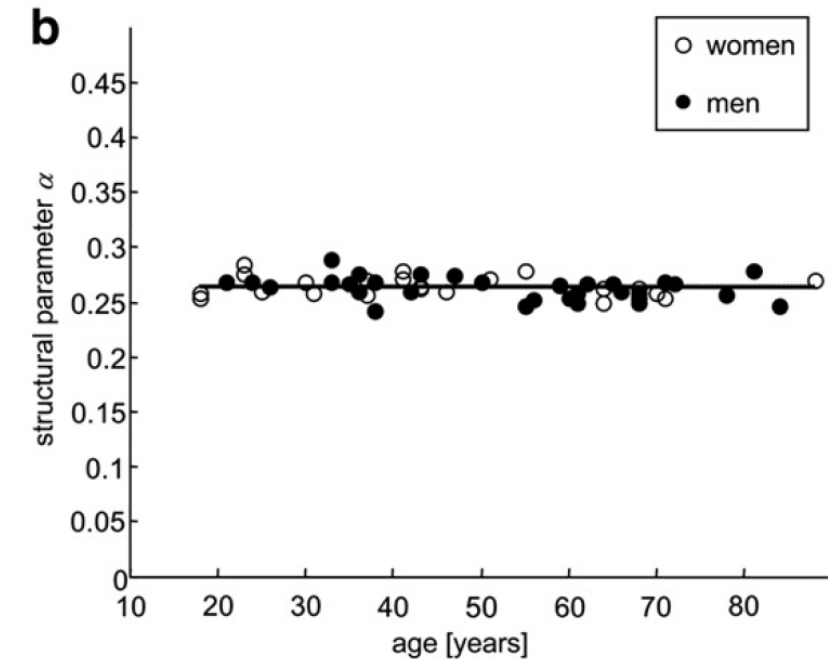
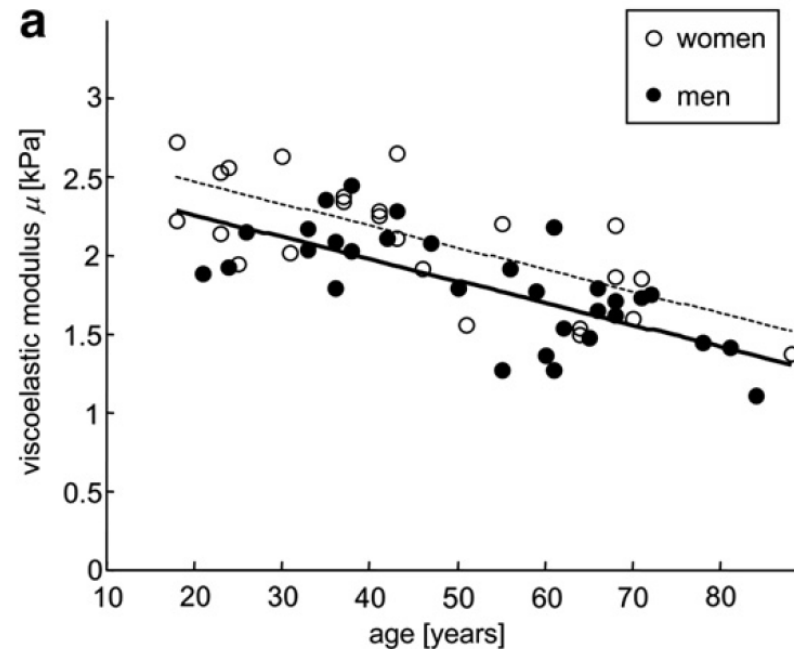
Kaspar-Josche Streitberger, et al PLOSOne 2012

$\mu \equiv$  reflects the cellular strength and connectivity of the tissue (units in KPa)

$\alpha \equiv$  reflects the complexity of the tissue network - porosity, permeability

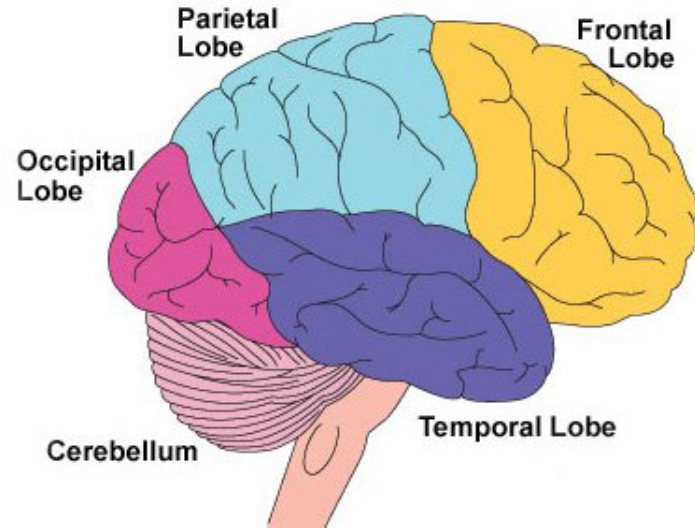
# Effect of age and gender on brain stiffness ( $\mu$ and $\alpha$ )

- Healthy adult brain undergoes steady parenchymal ‘liquefaction’ characterized by a continuous decline in  $\mu$  of 0.8% per year, whereas  $\alpha$  remains unchanged.
- Furthermore, significant sex differences were found with female brains being on average 9% stiffer (more solid-like) than their male counterparts

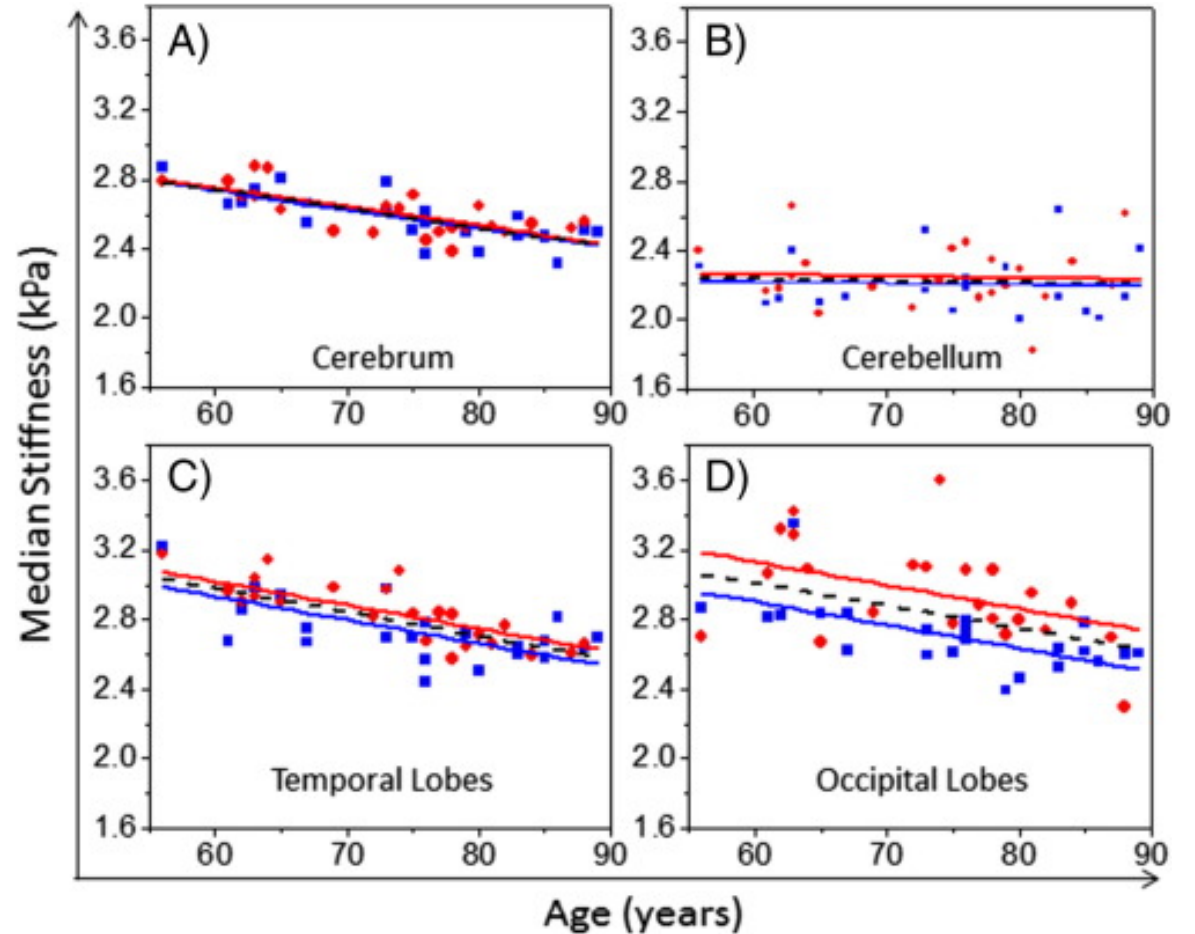


# Effect of age and gender on brain stiffness

Arani *et al* (2015) *NeuroImage* 111 (2015) 59–64



- Significant linear correlation between age and brain stiffness in cerebrum, frontal, occipital, parietal and temporal lobes



# MRE measurements in iNPH Streitberger *et al* (2010)

- 25% lower  $\mu$  in NPH patients compared to healthy control participants. There was also a significant reduction in  $\alpha$ , 9%, (both  $p < .001$ )

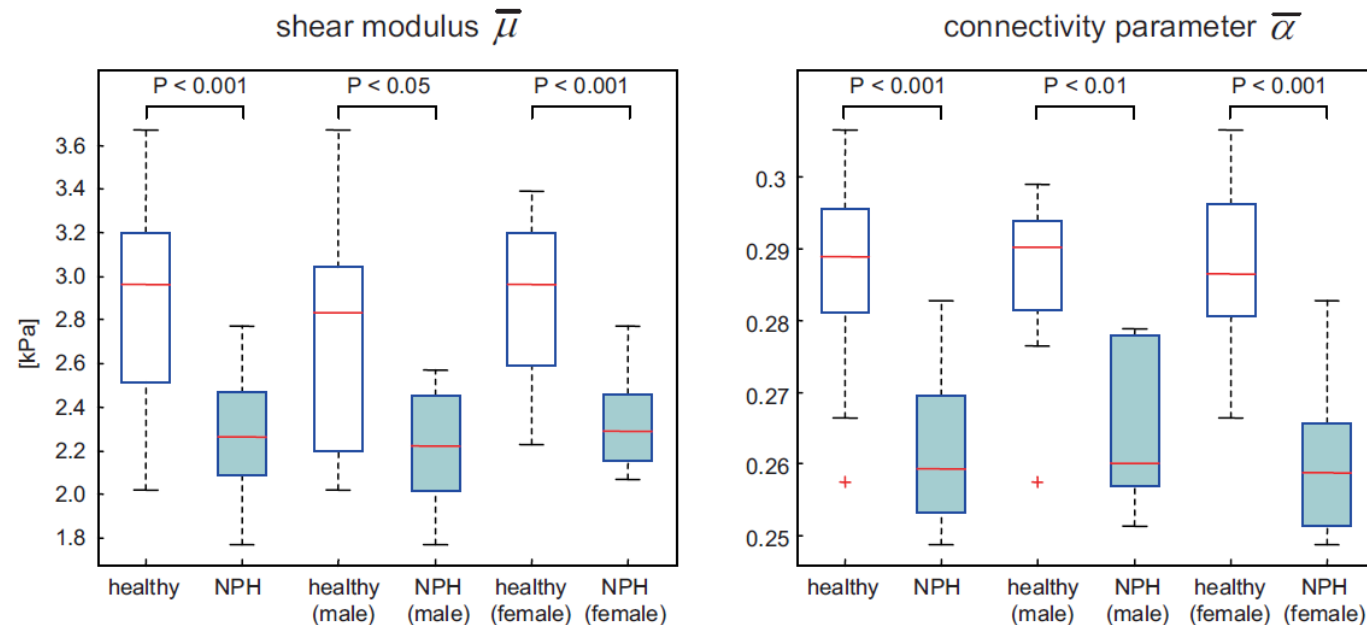


**Figure 3.** Patients with normal pressure hydrocephalus (NPH) present a global reduction in shear elasticity  $\bar{\mu}$  on the order of 20%. A similar loss of brain stiffness is seen in the subgroups of male and female patients. The connectivity parameter  $\bar{\alpha}$  is decreased in patients (−9%), corresponding to a reduction in wave energy loss and a transition of viscous brain tissue towards an elastic body.

# MRE measurements of $\mu$ and $\alpha$ in NPH Freimann *et al* (2012)

- The viscoelastic parameters  $\mu$  and  $\alpha$  were found to be decreased with  $-26\%$  and  $-10\%$ , respectively, compared to age-matched controls
- Interestingly,  $\alpha$  increased after shunt placement ( $P < 0.001$ ) to almost normal values whereas  $\mu$  remained symptomatically low.

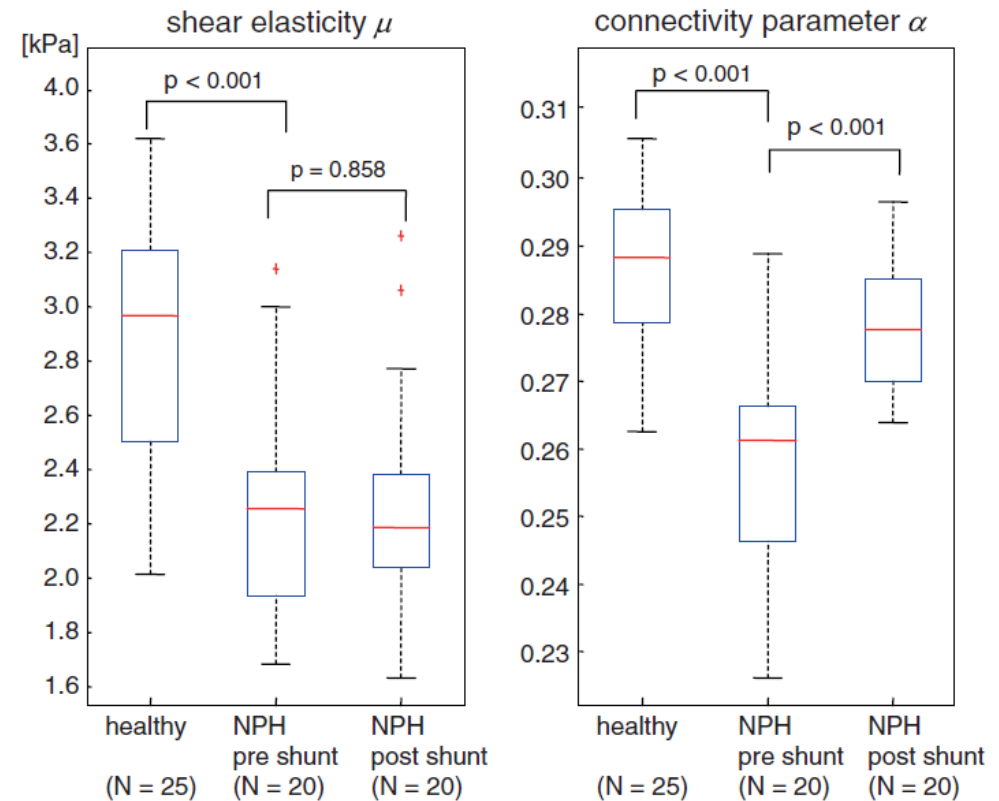
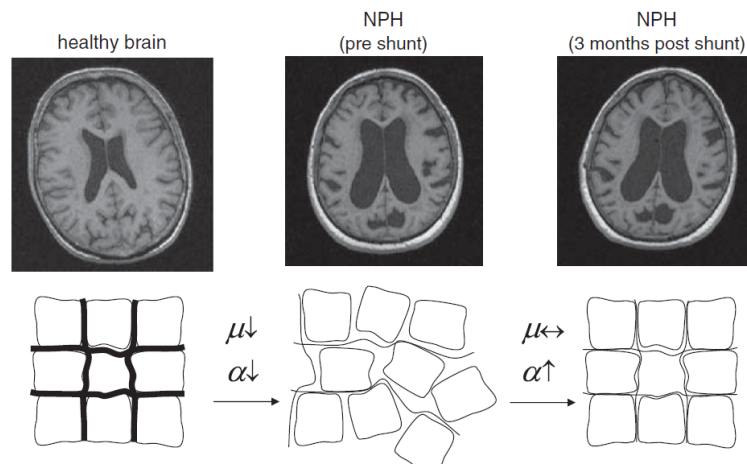
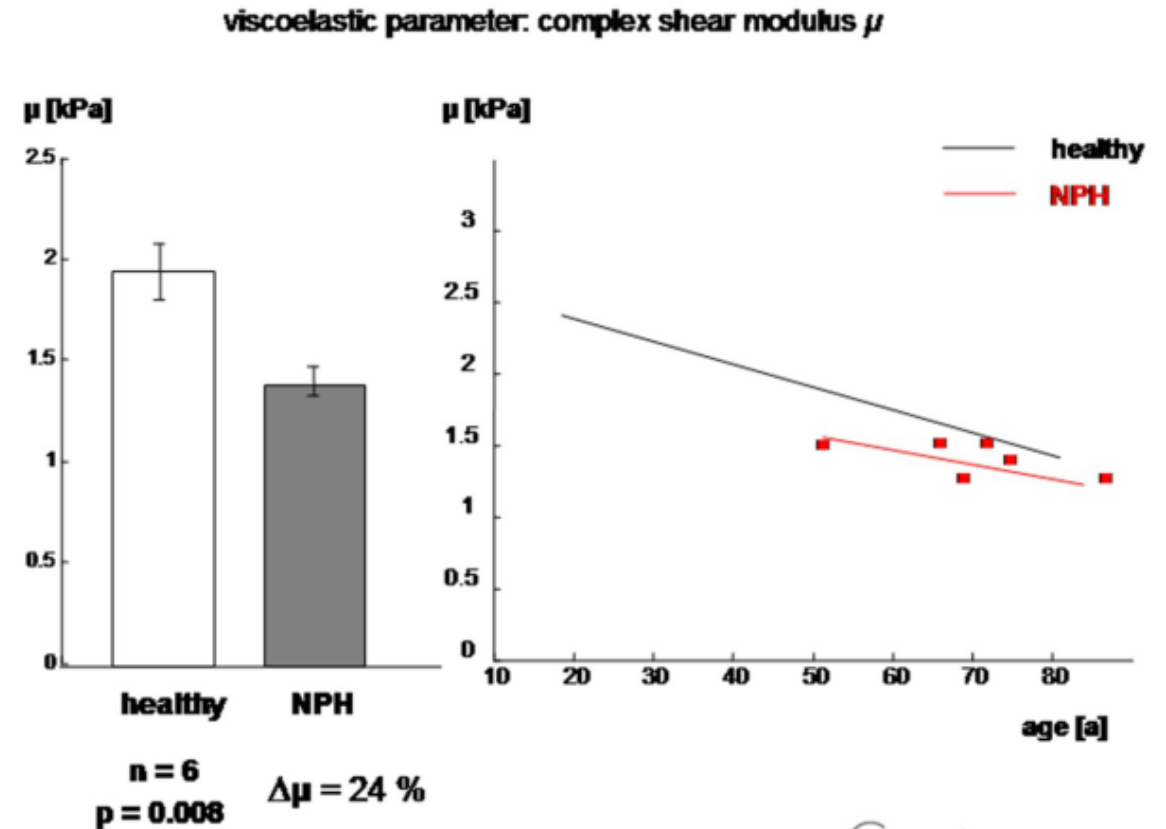


**Fig. 2** Brain viscoelastic parameters  $\bar{\mu}$  and  $\bar{\alpha}$  according to the springpot model in healthy volunteers (data taken from [17]) and in NPH prior and after shunting. The *boxplot* depicts the lower and upper quartiles as well as the 50th percentile (median). Full data range is presented by the *whiskers*

# MRE measurements of $\mu$ and $\alpha$ in iNPH patients Weiner et al 2010

- E. Wiener *et al* (2010): “Changes in viscoelastic brain tissue properties of patients with normal pressure hydrocephalus measured by MR elastography”
  - Six patients (mean age of 70.5 years) with the clinical diagnosis of NPH and six age-matched healthy volunteers (mean age of 69.2 years)
  - Inversion: Multifrequency- springpot model (same as Streitberger *et al* (2010) and Freimann *et al* (2012))
  - A **decrease (24%) of cerebral viscoelasticity** in patients with NPH ( $\mu = 1.47$  kPa) compared to age-matched healthy volunteers ( $\mu = 1.95$  kPa)



## Clinical Correlation of Abnormal Findings on Magnetic Resonance Elastography in Idiopathic Normal Pressure Hydrocephalus

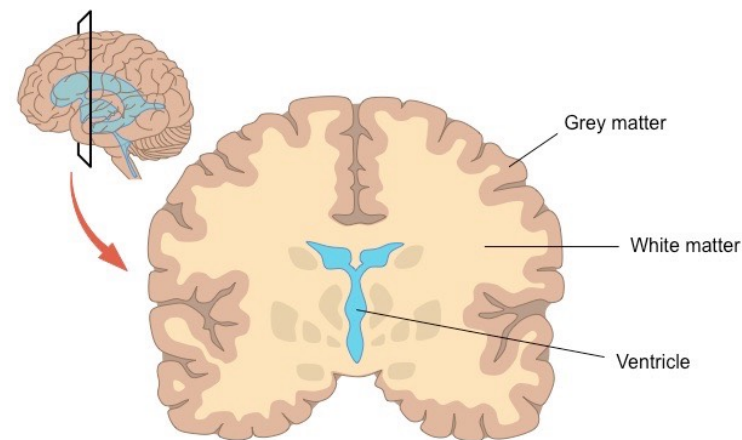
Avital Perry<sup>1</sup>, Christopher S. Graffeo<sup>1</sup>, Nikoo Fattahi<sup>2</sup>, Mona M. ElSheikh<sup>2</sup>, Nealey Cray<sup>1</sup>, Arvin Arani<sup>2</sup>, Richard L. Ehman<sup>2</sup>, Kevin J. Glaser<sup>2</sup>, Armando Manduca<sup>3</sup>, Fredric B. Meyer<sup>1</sup>, John Huston III<sup>2</sup>

WORLD NEUROSURGERY 99: 695-700, MARCH 2017

**Table 2.** Brain Stiffness in Idiopathic Normal Pressure Hydrocephalus Patients and Healthy Controls

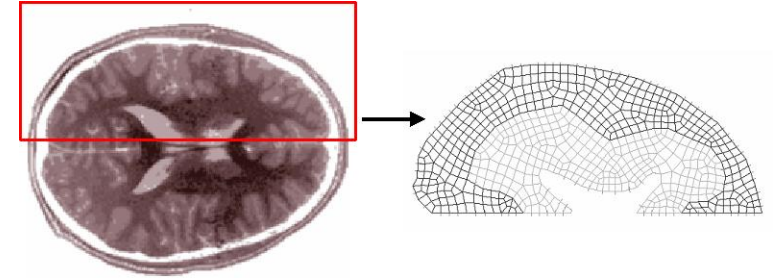
Region of Interest	iNPH Group (n = 10)	Control Group (n = 20)	P Value
Cerebrum	2.64 ± 0.11	2.55 ± 0.11	0.04
Frontal	2.65 ± 0.05	2.74 ± 0.03	0.1
Occipital	2.97 ± 0.15	2.75 ± 0.16	0.002
Parietal	2.63 ± 0.18	2.45 ± 0.12	0.01
Temporal	2.79 ± 0.48	2.73 ± 0.03	0.3
Deep gray	2.91 ± 0.09	3.00 ± 0.06	0.4
Cerebellum	2.20 ± 0.04	2.23 ± 0.03	0.6
Periventricular	1.74 ± 0.24	2.26 ± 0.29	<0.0001

Corrected stiffness reported as mean ± standard error.  
iNPH, idiopathic normal pressure hydrocephalus.



**A reduction in the stiffness is mainly localized in the periventricular WM where a reduction of 23% is measured (p< 0.0001)**

# Grey and white matter results



- WM was found to be more viscous than GM in all studies, as demonstrated by the loss tangent

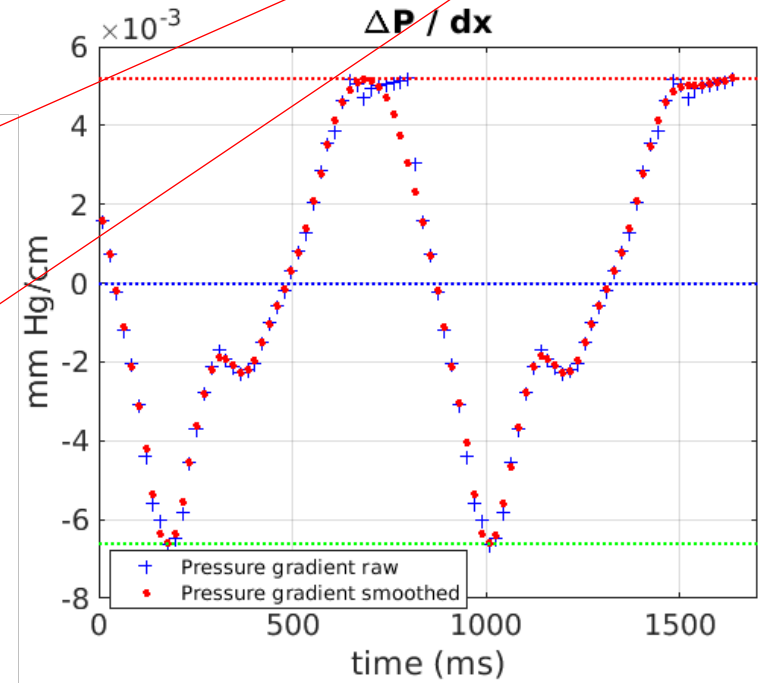
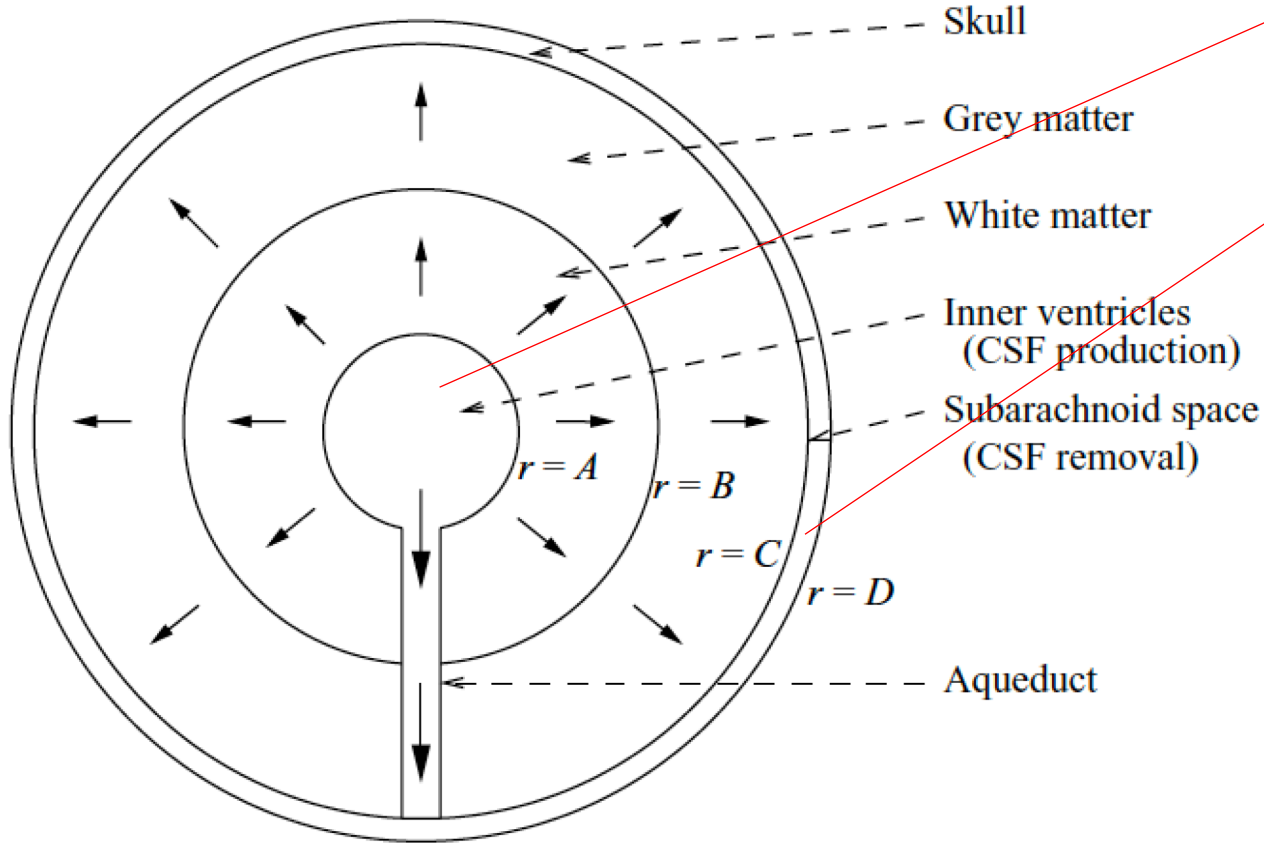
Author	N	Approach	$f$ in Hz	GM		WM	
				Shear stiffness (kPa)	Loss tangent (rad)	Shear stiffness (kPa)	Loss tangent (rad)
Braun <i>et al</i> (2014)	5	MDEV	30, 40, 50, 60	$0.98 \pm 0.25$	$0.95 \pm 0.03$	$1.16 \pm 0.29$	$1.03 \pm 0.04$
Johnson <i>et al</i> (2013a)	3	NLI	50	$2.01 \pm 0.08$	$0.37 \pm 0.18$	$2.86 \pm 0.13$	$0.46 \pm 0.15$
Johnson <i>et al</i> (2013b)	7	NLI	50	$2.41 \pm 0.19$	$0.48 \pm 0.17$	$3.30 \pm 0.35$	$0.52 \pm 0.20$
Clayton <i>et al</i> (2012)	5	LFE	60	$3.77 \pm 0.50$	$0.50 \pm 0.27$	$4.16 \pm 0.17$	$0.54 \pm 0.08$
McCracken <i>et al</i> (2005)	6	DI	80	$5.30 \pm 1.30$	n/a	$10.70 \pm 1.40$	n/a
Zhang <i>et al</i> (2011)	8	DI	80	$2.72 \pm 0.22$	$0.44 \pm 0.14$	$2.85 \pm 0.36$	$0.47 \pm 0.28$
Green <i>et al</i> (2008)	5	DI	90	$4.48 \pm 0.31$	$0.68 \pm 0.10$	$4.24 \pm 0.31$	$0.75 \pm 0.10$
Kruse <i>et al</i> (2008)	25	LFE	100	$5.22 \pm 1.15$	n/a	$13.60 \pm 3.19$	n/a

*Note.* Values show mean  $\pm$  standard deviation (SD). n/a = not available.

Published values for each study can be found in table 2 of appendix 2 in the supplementary material.

# Proof of concept simplified geometry

Transmantle pressure  $P_t = P_v - P_{SAS}$



$$\sigma(t) = \mu^{1-\alpha} \eta^\alpha \frac{\partial^\alpha \epsilon}{\partial t^\alpha}$$

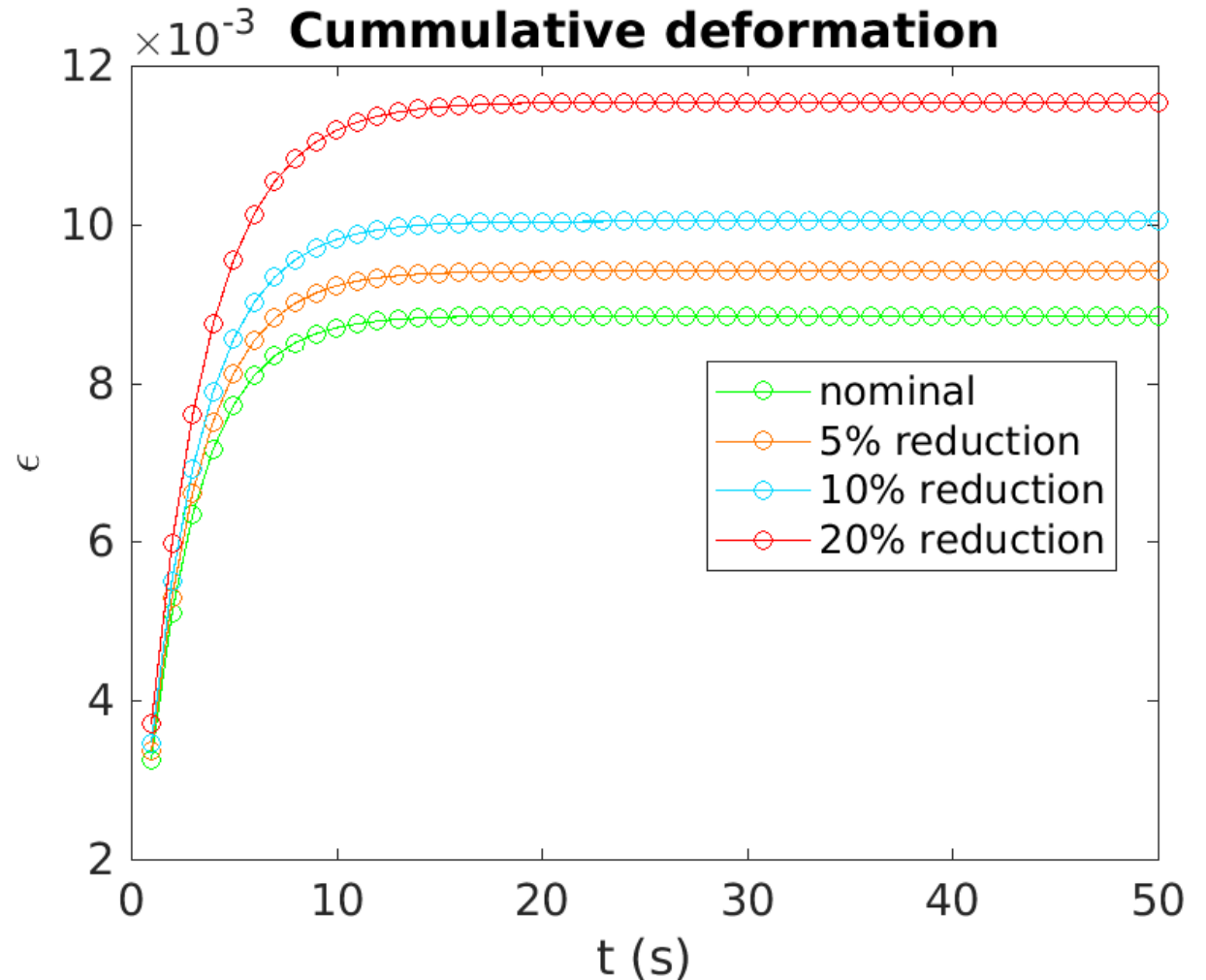
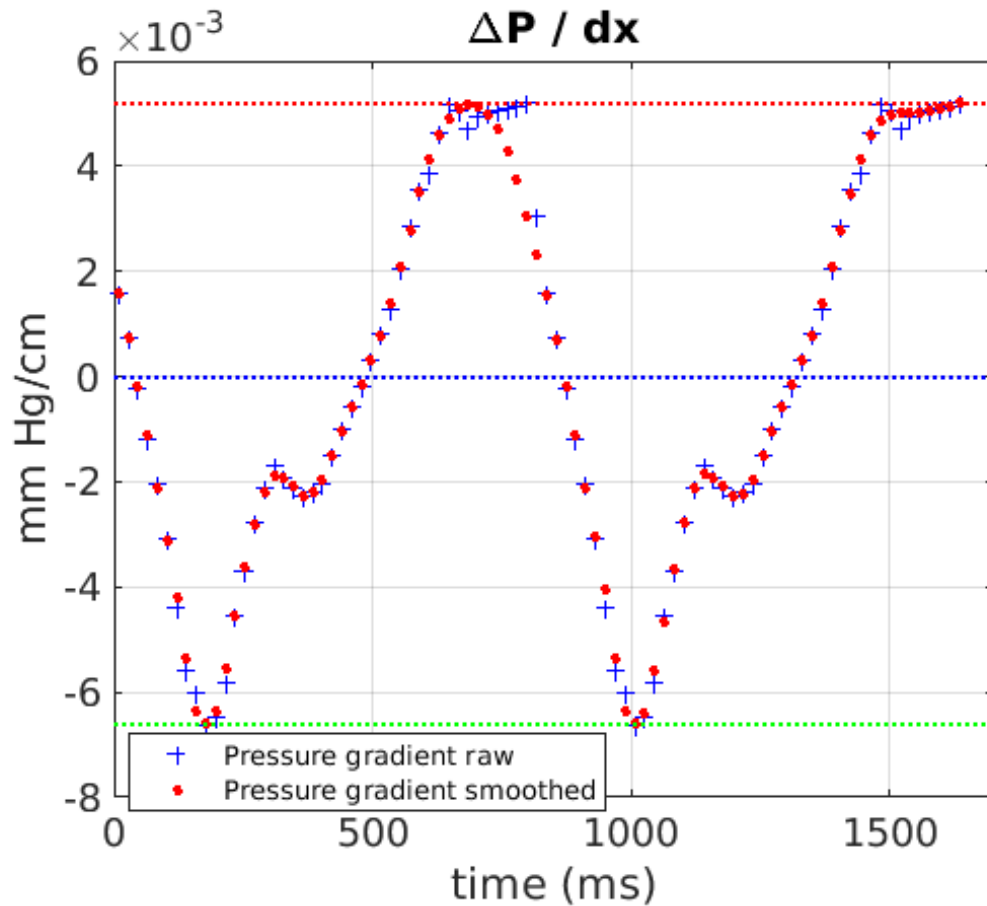
$\sigma$  = stress

$\eta$  = viscosity  $\equiv 3.7$  Pa (water)

$\epsilon$  = strain

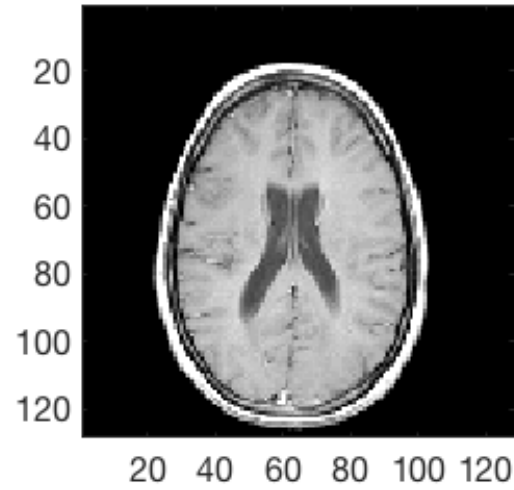
The ventricles undergo a gradual permanent enlargement as  $\mu$  of the WM is decreased 5%, 10%, or 20% while maintaining the mean ICP constant and the time variation of the transmural pressure

Transmantle pressure  $dP_t = P_{\max} - P_{\min} = 0.0578$  mmHg

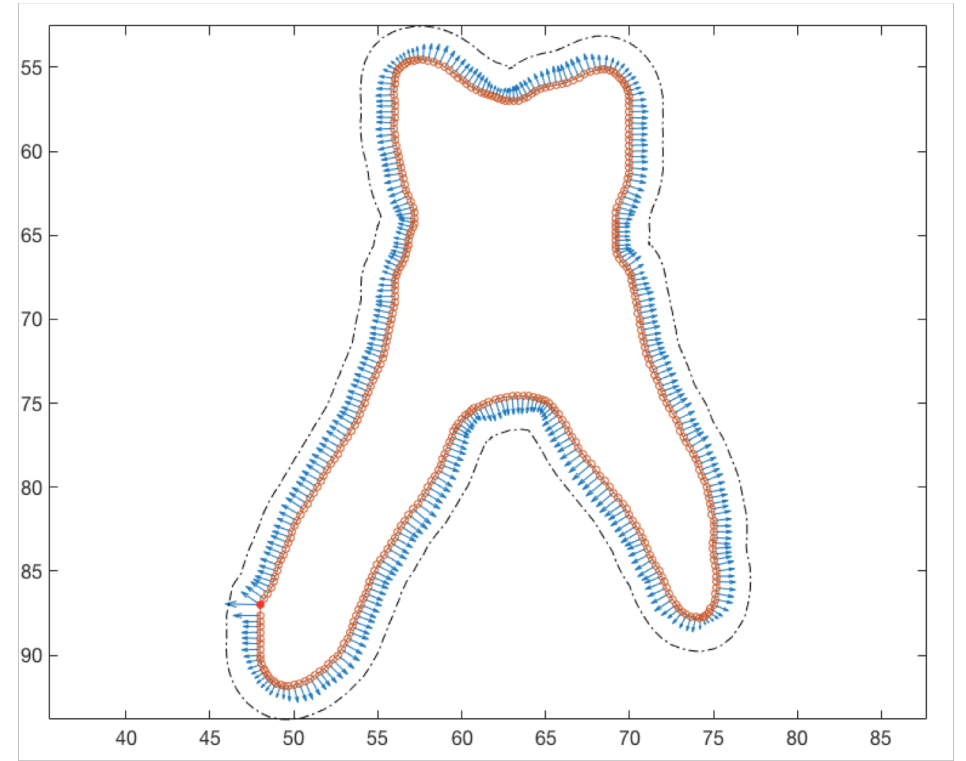
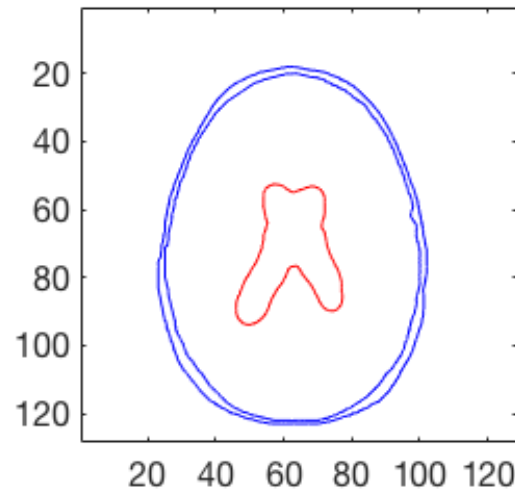
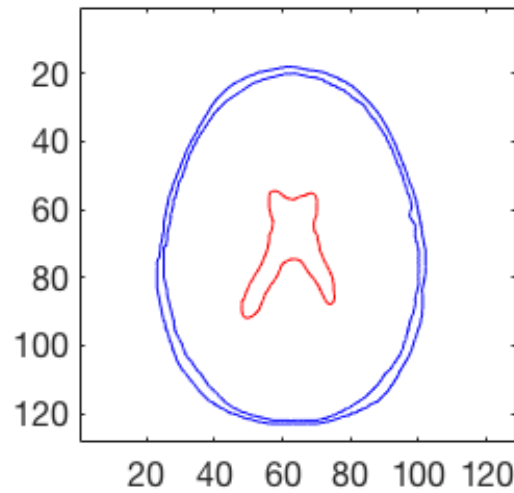
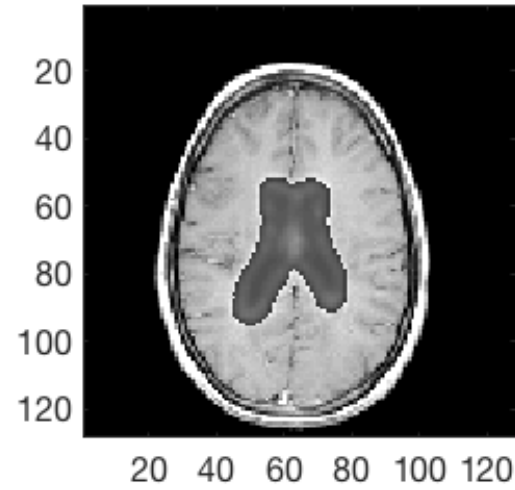


# iNPH simulation

Normal

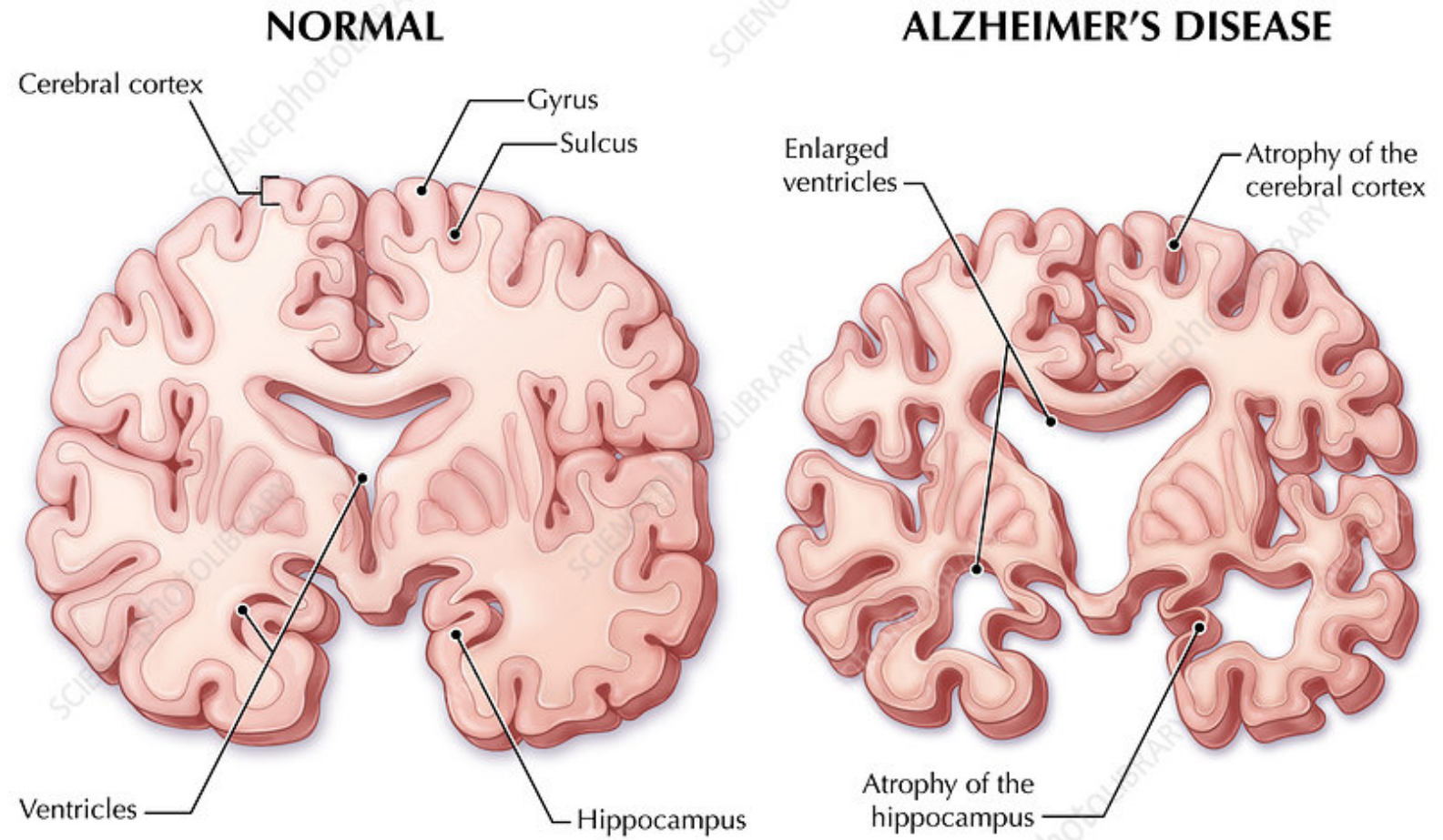


NPH



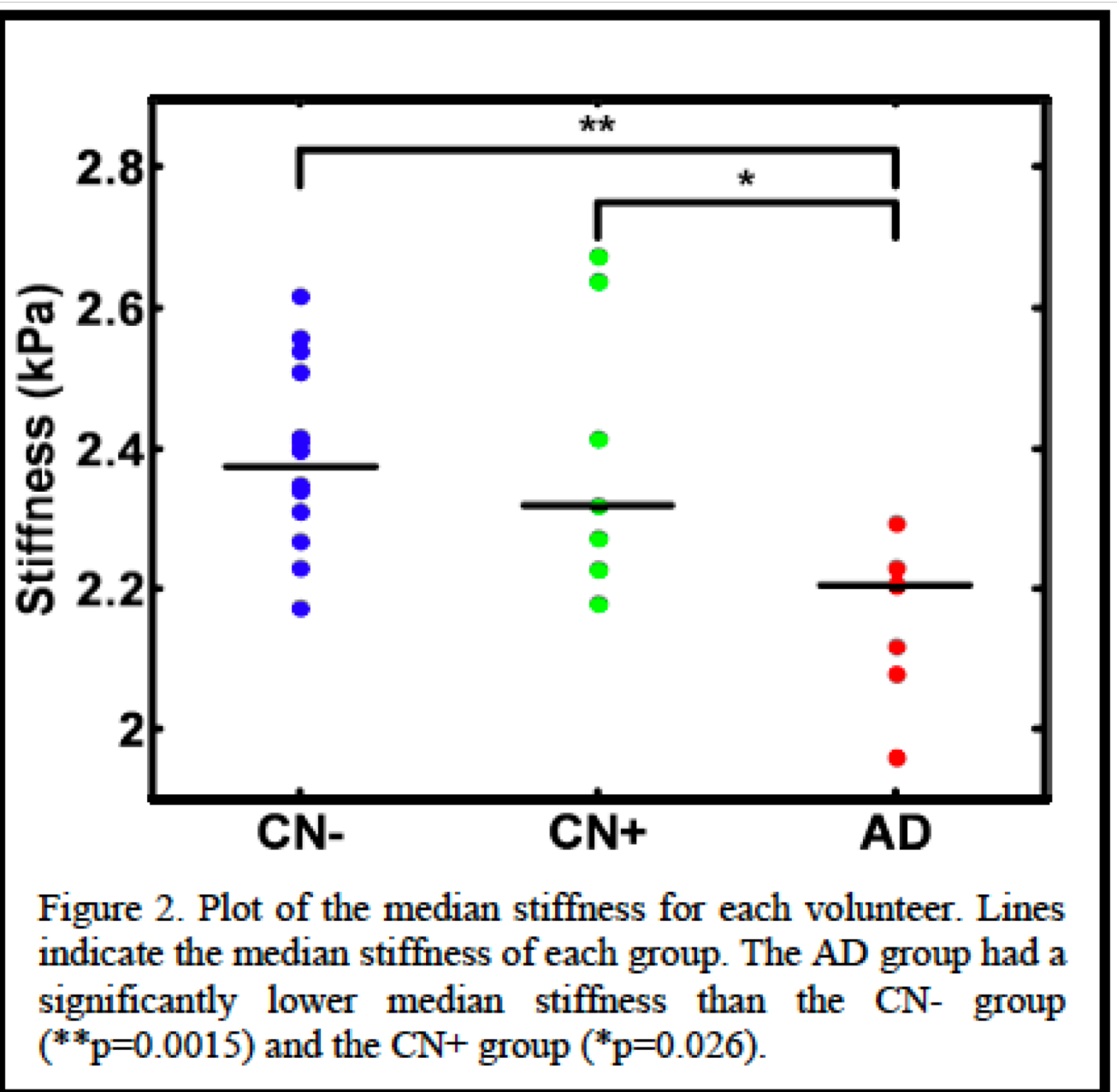
In **Alzheimer's** disease, there is an overall shrinkage of brain tissue.

In addition, the **ventricles** are noticeably **enlarged**.



Amyloid-negative cognitively normal controls (CN-),  
Amyloid-positive (PIB SUVR >1.5) cognitively normal controls (CN+),  
Amyloid-positive (PIB SUVR >1.5) subjects with probable Alzheimer's disease (AD).

Murphy et al. Proc. Intl. Soc. Mag. Reson. Med. 19 (2011)



# Take Home message and Concluding Thoughts

- We have proposed the hypothesis that gradual changes in the elasticity ( $\mu$ ) and/or permeability (porosity) ( $\alpha$ ) of the periventricular white matter (WM) may lead to a slow gradual enlargement of the ventricles (residual strain) without an increase in the mean intracranial pressure (ICP)
- A computational model that incorporates measurements of the transmante pressure as well as recent MRE measurements of the changes in the viscoelastic properties of the brain tissue demonstrates that a decrease in the elasticity of the periventricular WM leads to a gradual enlargement of the ventricles while the ICP remains constant.
- Our analysis indicate that age and gender should also be considered as a cause of iNPH
  - To what extent is the age related degeneration of the brain elasticity accelerates iNPH?
  - If there is a marked difference in stiffness between sexes then how would this affect the progression of iNPH in female vs males?

# Take Home message and Concluding Thoughts

- The iNPH progresses insidiously over long periods of times, presumably over several months, or even years. There is a need for an early detection which will enable intervention (surgically or pharmacologically) that could stop or reverse the symptoms before brain atrophy had occurred.
- What physiological parameters (i.e., cardiac rate, high blood pressure, breathing disorders, etc.) accelerate the changes in  $\mu$  and  $\alpha$  in some patients?
- What are the specific biochemical changes in the protein composition and/or cellular structure of the brain parenchyma that causes the decrease in  $\mu$  in INPH patients? Deep white matter ischemia characterized histologically by myelin pallor (i.e., loss of lipid). The attraction between the bare myelin protein and the CSF increases resistance to the extracellular outflow of CSF (decrease permeability  $\alpha$ ).
- Identification of these biochemical markers could lead to an early detection and surgical treatment of iNPH (before atrophy).



Victor Haughton, School of Medicine. U Wisconsin-Madison



Kevin King. Huntington Medical Research Institutes, Pasadena



Antonio Sánchez, University of California San Diego



Carlos Martínez-Bazan. Universidad de Jaen, Spain

J. J. Lawrence, W. Coenen, C. Gutiérrez-Montes, E. Criado-Hidalgo, Stephanie Sincomb,, Ke Wei